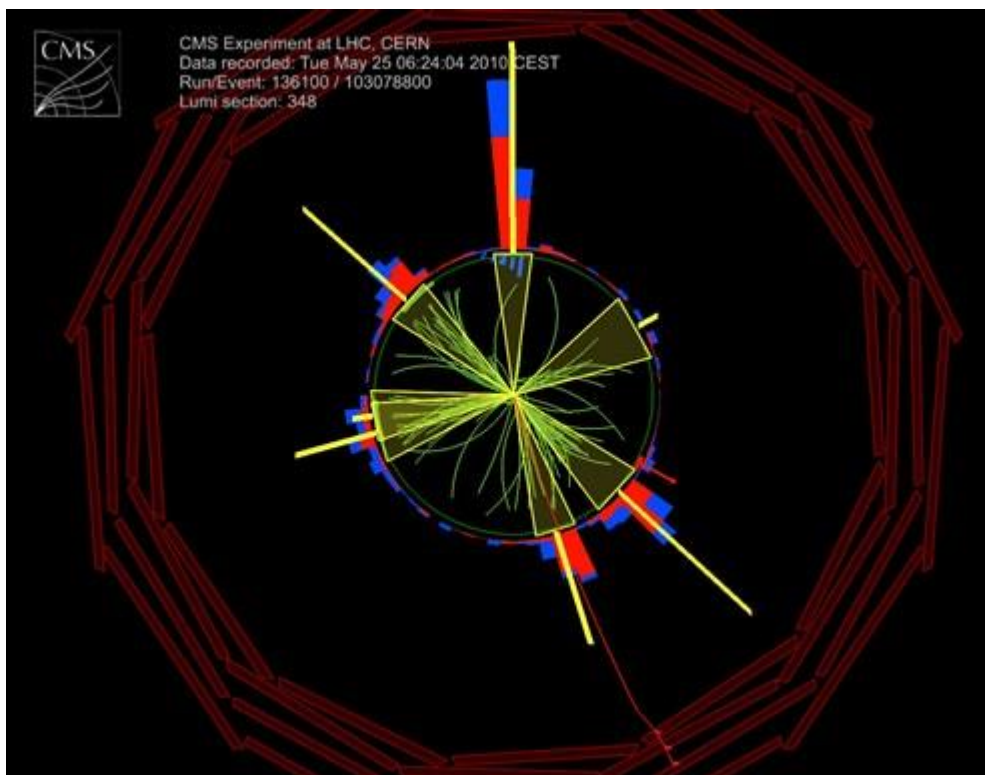


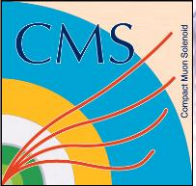
CMS QCD physics results

Olga Kodolova, SINP MSU
on behalf of the CMS Collaboration



Outline

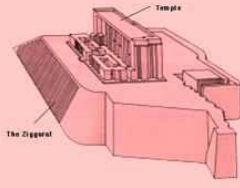
- **Motivation**
- **Scope of studies**
- **Soft physics**
- **Hard physics**
- **Summary**



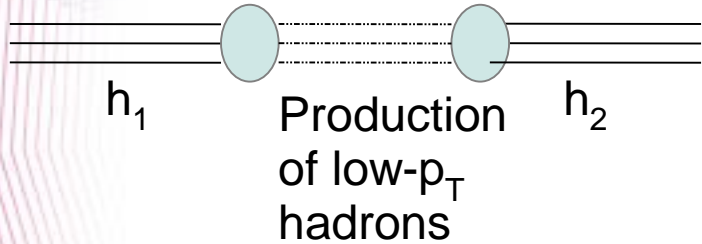
Motivation

- QCD is the constituent of the Standard Model which deals with strong interactions
- The verification of the QCD validity is the first step towards the new Physics.
 - QCD processes are background to the Higgs production, SUSY, many BSM models, rare processes that are scope of the Standard Model itself
 - QCD defines the hadronization process of partons whatever interaction mediator is in the hard production vertex

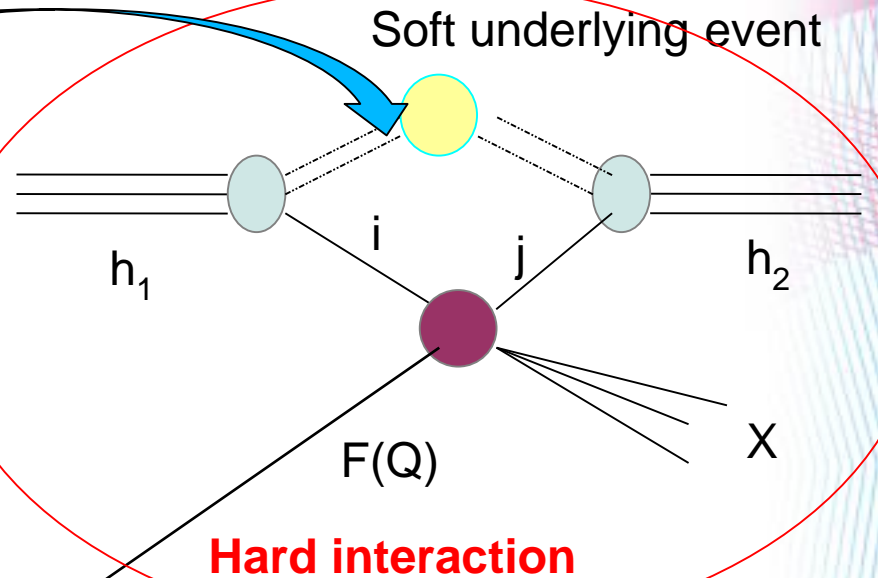
QCD at hadron colliders



In hadron collisions all phenomena are QCD related but we should distinguish between Soft and Hard physics.



Soft interaction: nQCD



Factorization theorem

$$\sigma(P_{h_1}, P_{h_2}) = \sum_{i,j} \int dx_1 dx_2 f_{i/h_1}(x_1, \mu_F^2) f_{j/h_2}(x_2, \mu_F^2) \hat{\sigma}_{ij}(p_1, p_2, \alpha_S(\mu_R), Q^2; \mu_F^2, \mu_R^2)$$

$$p_1 = x_1 * P_1, p_2 = x_2 * P_2$$

Parton distribution function (PDF)

Partonic cross-section computed in pQCD

μ_F – factorization scale separates long and short distance physics

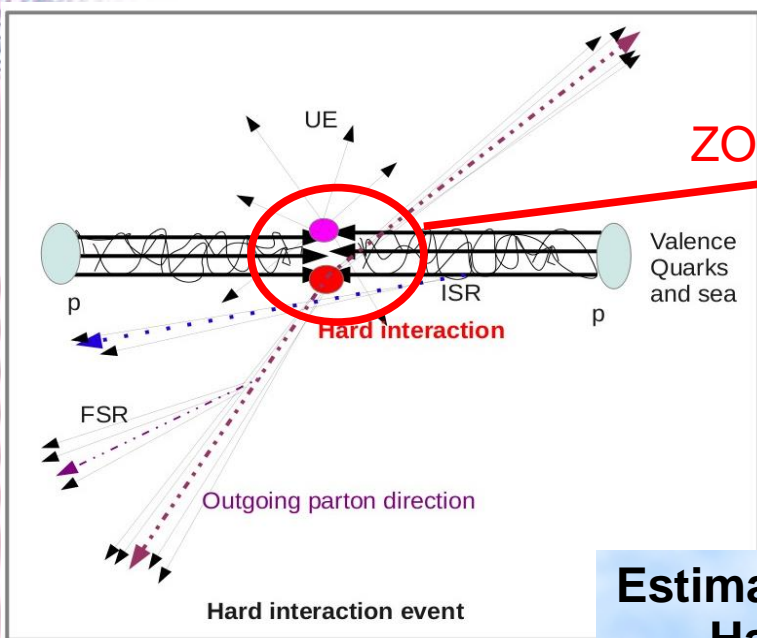
$\alpha_S(\mu_R)$ – running coupling constant

$Q^2 = -q^2$ – transferred momentum

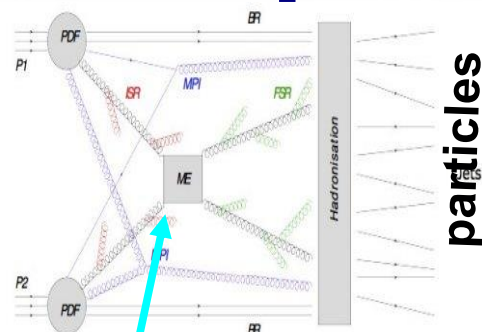
$$\hat{\sigma}_{ij} = \alpha_S^k \sum_n \left(\frac{\alpha_S}{\pi}\right)^n \sigma_{ij}^n$$

Lattice calculation
Fixed-order QCD: LO, NLO, NNLO + PS

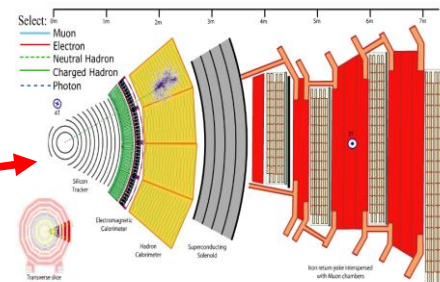
How do we proceed



ZOOM



2 step unfolding meet at particles level



Reconstructed particles, reconstructed jets

Differential Cross-sections

Multiplicity

Rapidity

Momentum of Particles and Jets, missing E_T

Estimate:

- Hard interaction cross-section
- Parton Distribution Functions
- Parton showering details

Theory approximations

Perturbative QCD (pQCD):

LO, NLO, NNLO calculations, ME + parton showering, threshold resummation

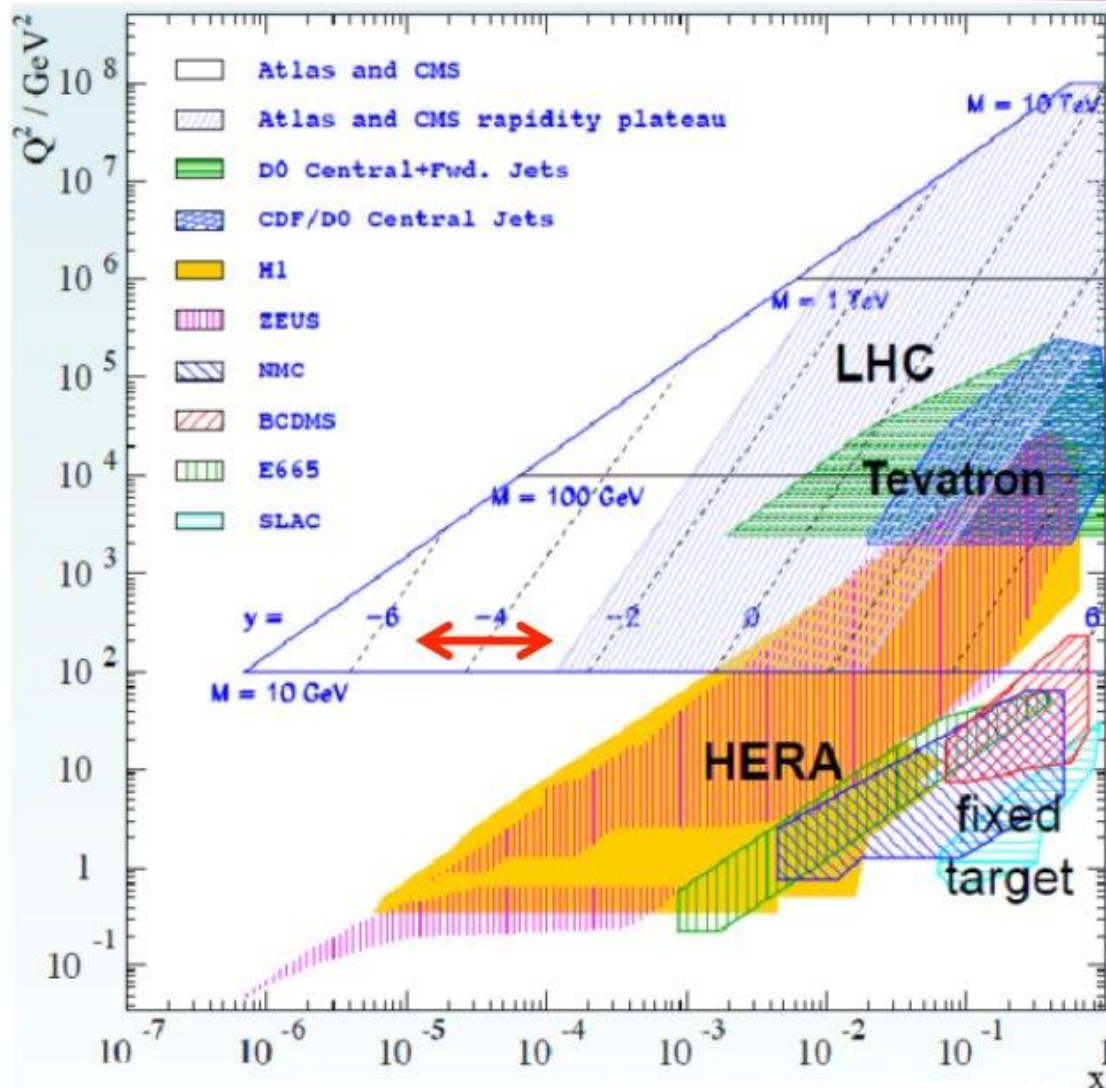
non-pQCD: (Multi-parton interactions (MPI), String/Cluster fragmentation models)

Where we are now

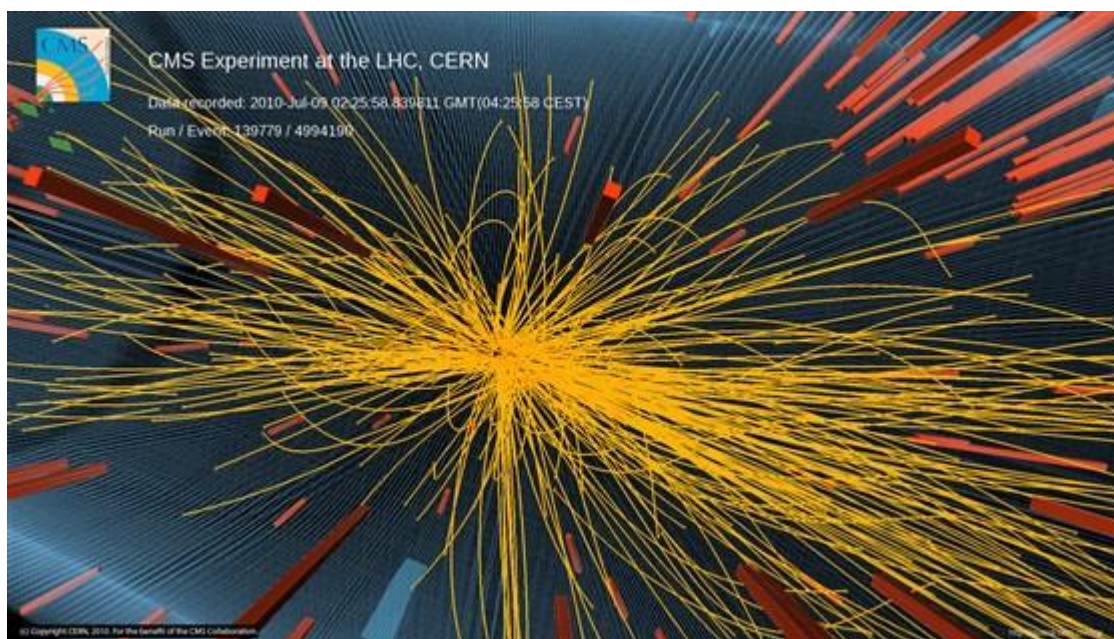
Probing the new territory
(x, Q^2) range

QCD is always present

Important background for new physics searches
enormous cross section: QCD
can hide many possible signals
of new physics

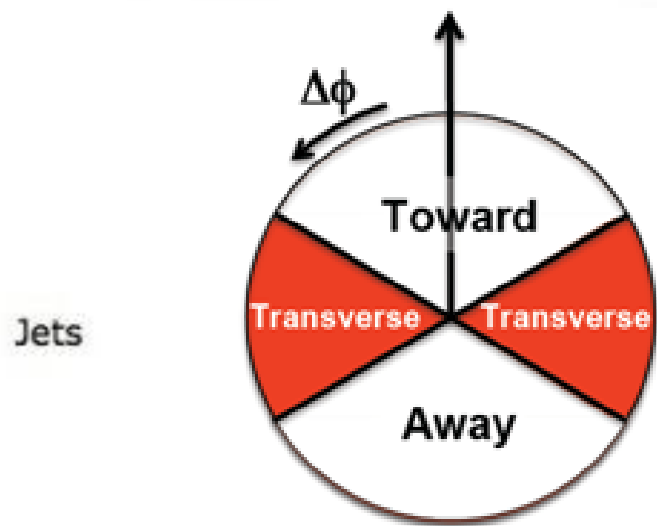
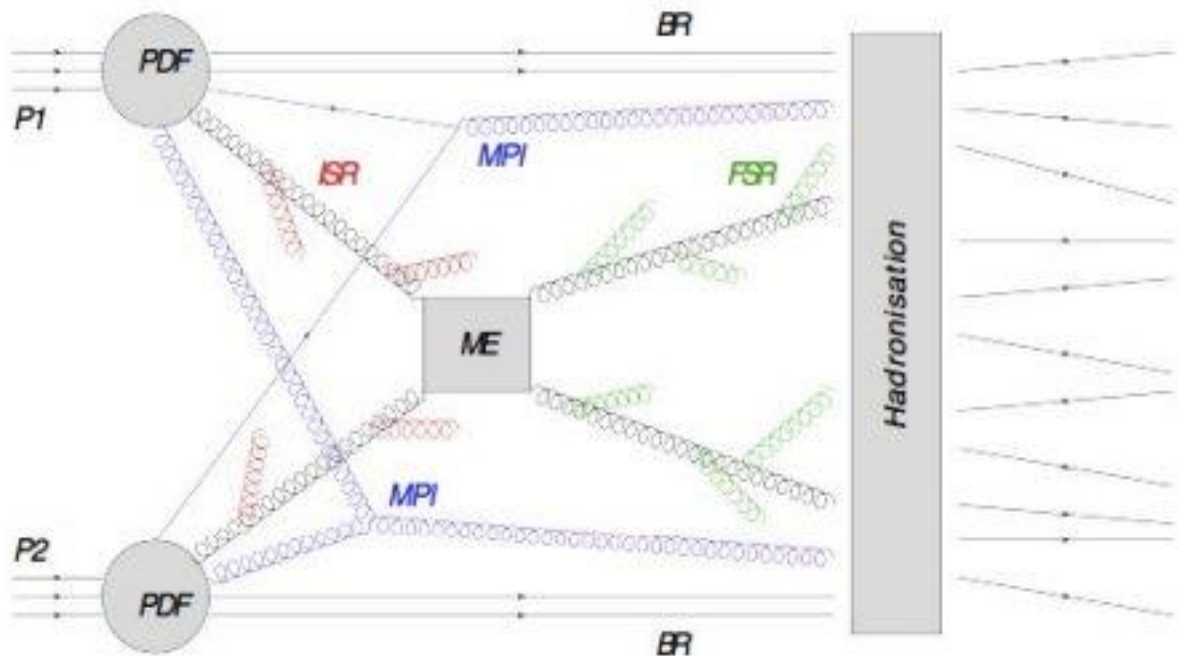


Soft particles production, Underlying event (UE)



Underlying event

Soft and hard components



Everything in event that is not hard interaction (ME): soft&semi-hard interactions which are not described with pQCD

Beam remnants (BR): what remains after the interacting partons left the hadron

Initial (ISR) and final (FSR) state radiation

Multiple Parton Interactions (MPI). If higher p_t interactions → Double Parton Scattering

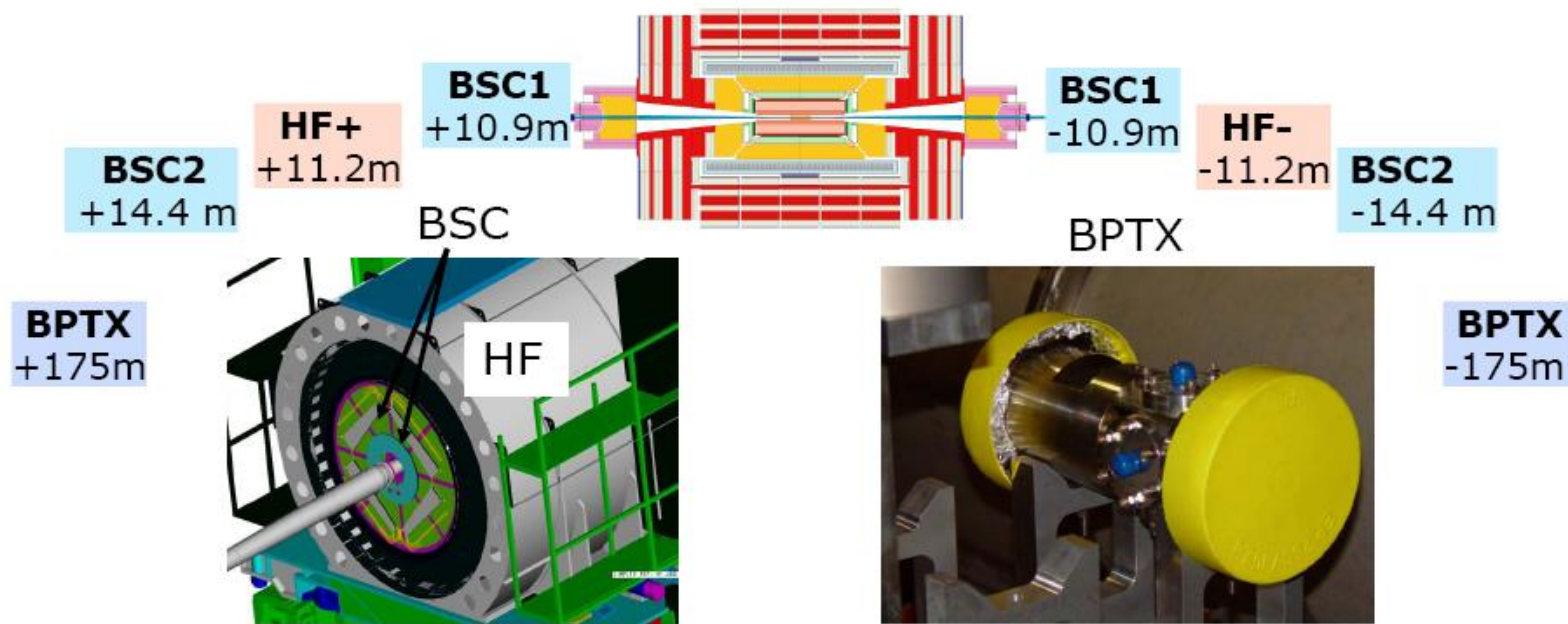
UE activity is typically studied in the transverse region in pp collisions as a function of the hard scale of the event, and at different centre-of-mass energies (\sqrt{s}):

Particle production in **MinBias events** or **events with high energy track or jet** (hadronic events)

Drell-Yan events

MinBias (MB) events selection

Trigger System



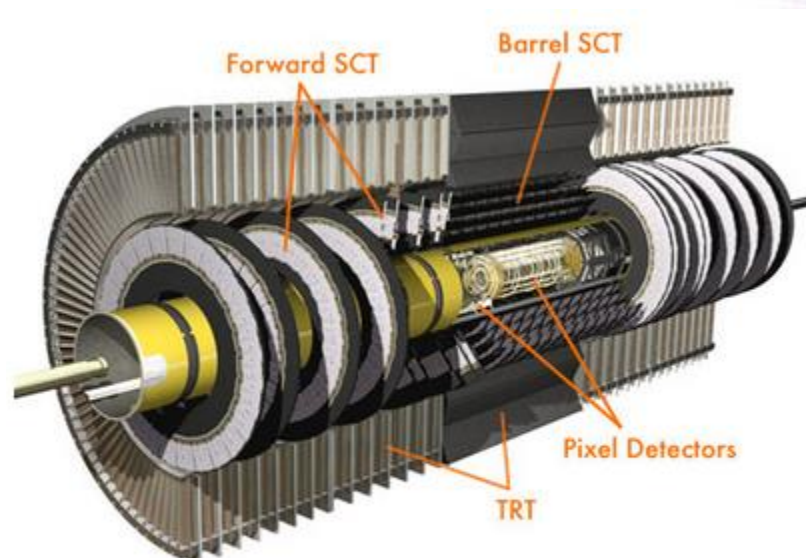
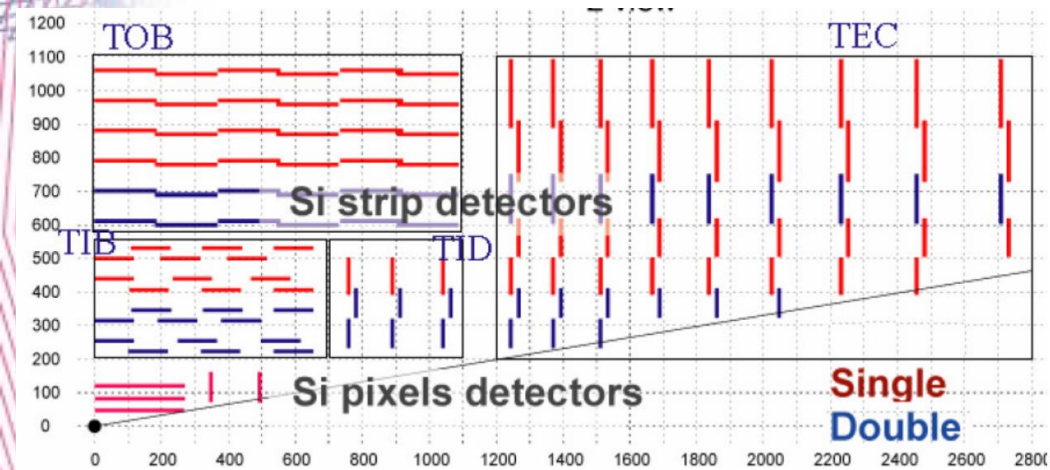
Trigger :

- Beam crossover
- Activities in forward calorimeters & scintillators

Offline event selection :

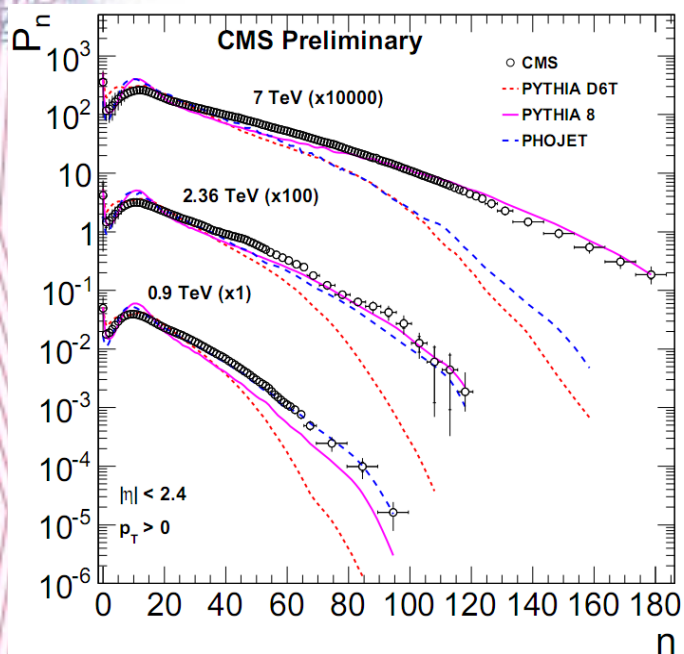
- rejection of the beam halo & beam background
- selection of main primary vertex
- some diffraction rejection cuts if needed

Charged particles reconstruction



- Acceptance $|\eta| < 2.5$
- Standard tracking down to 100 MeV
- Dedicated low p_T tracking used for some measurements
- Particles identification is available for low- p_T hadrons via energy losses in: pions, kaons, protons

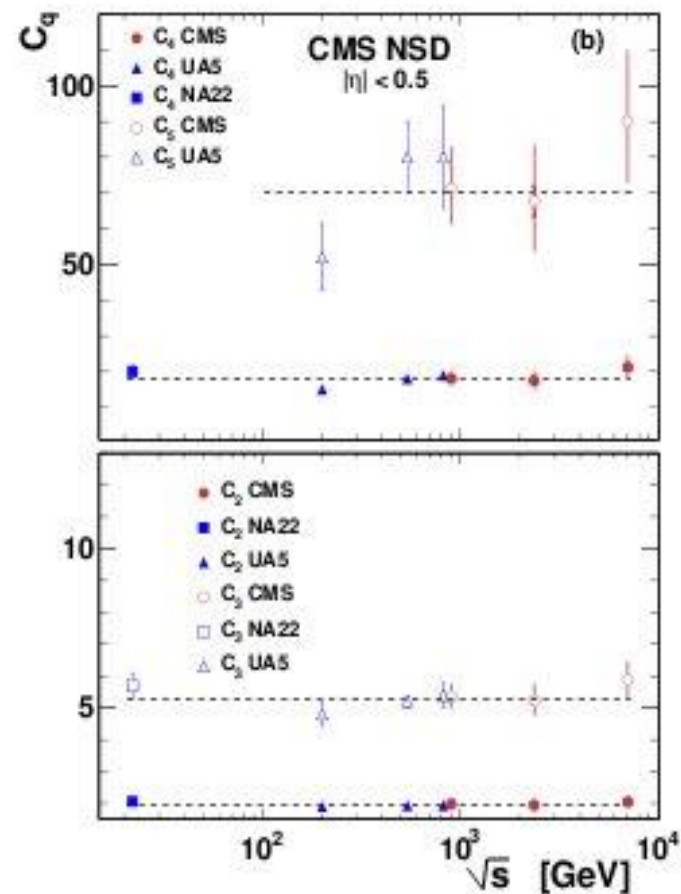
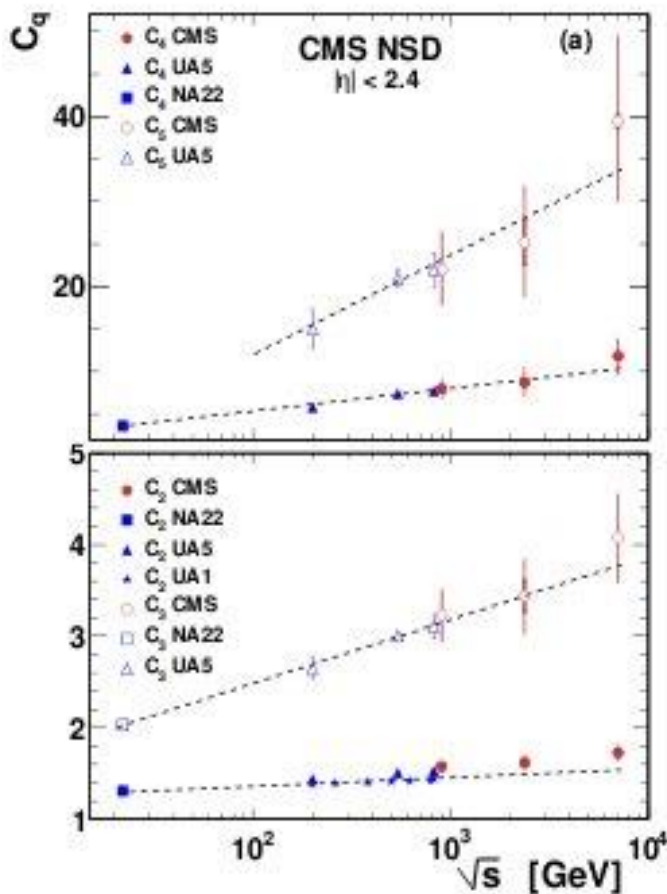
Charged particles multiplicity



Evidence of the multi-component structure (change of the slope at $n \sim 20$)

Violation of the KNO (Koba-Nielsen-Olesen) scaling ($z = n / \langle n \rangle$ distribution independent on collision energy) in the range $|\eta| < 2.4$

Still KNO scaling in the range $|\eta| < 0.5$



KNO scaling suppose the independence of C_q on the collision energy.

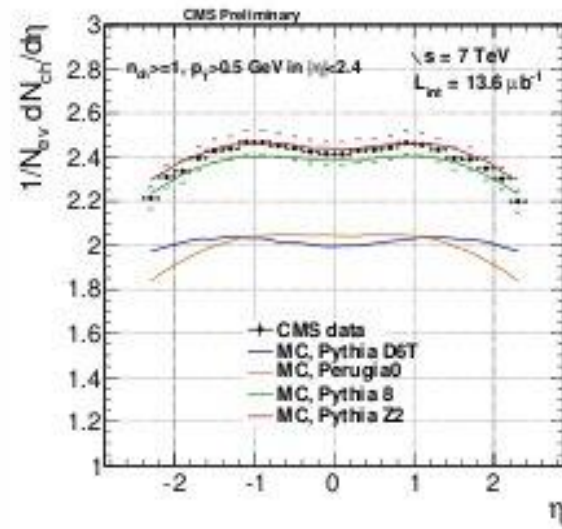
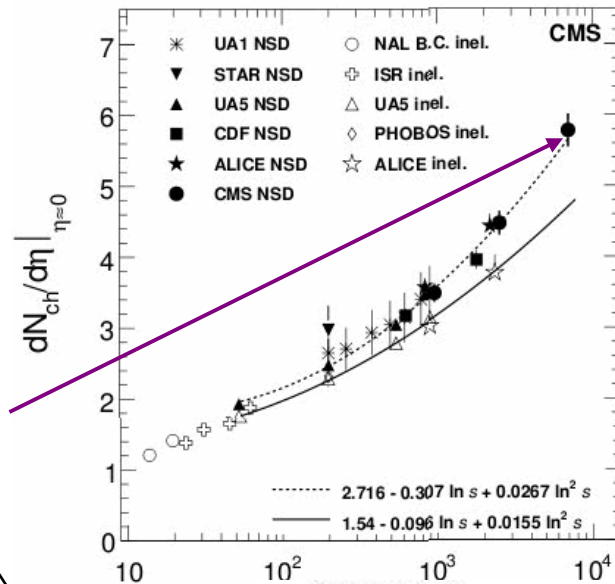
$$C_q = \frac{\langle n^q \rangle}{\langle n \rangle^q}$$

JHEP01(2011)079

Charged particles density p_T, η (0.9 TeV-8 TeV)

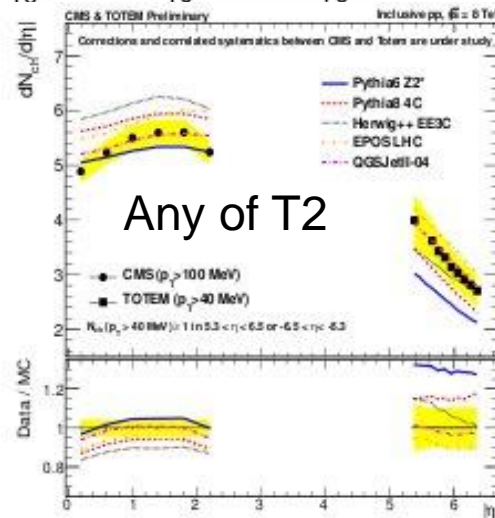
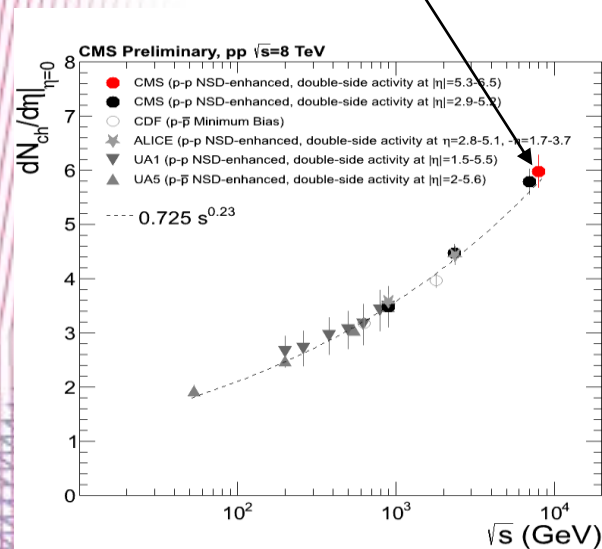
Measured NSD multiplicity is higher than most of the predicted:

new input to the dynamics of soft hadronic interactions

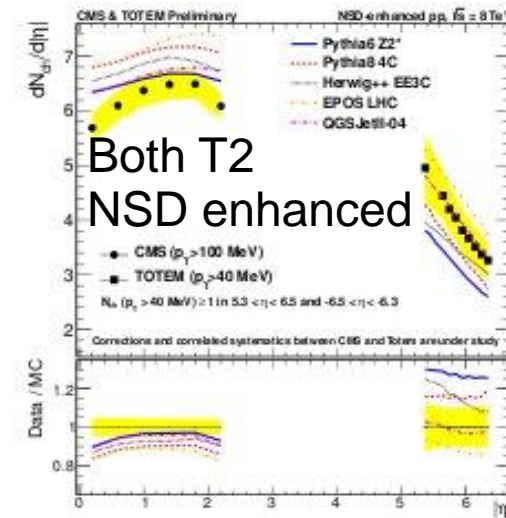


$p_T > 0.5$ GeV/c

PYTHIA 8 and Z2 describes η -distribution for low- p_T charged hadrons at 7 TeV



Any of T2

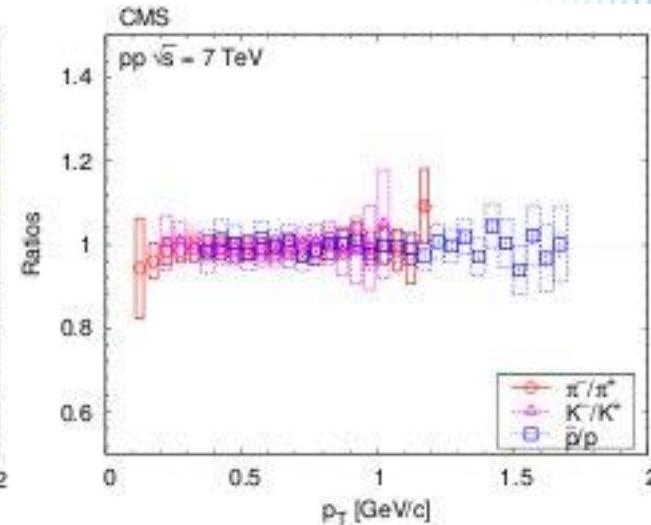
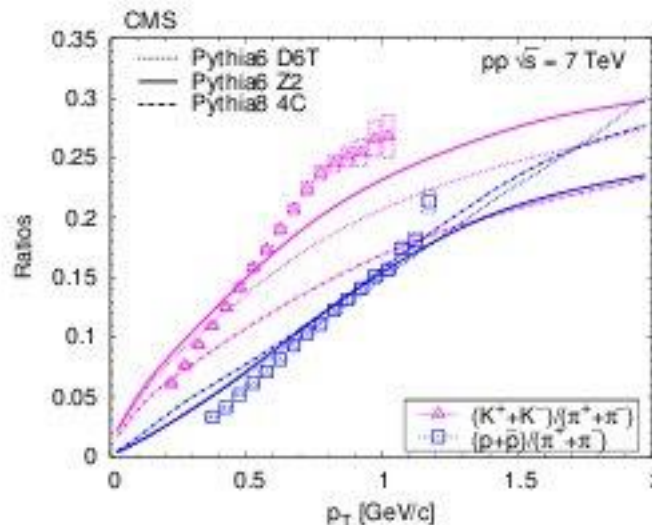
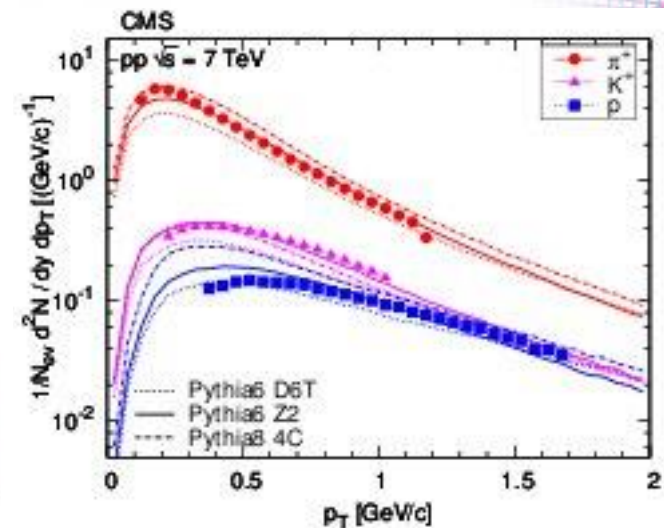
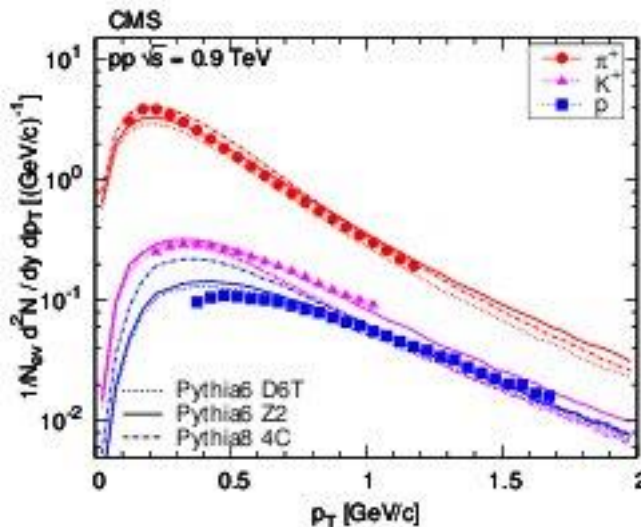
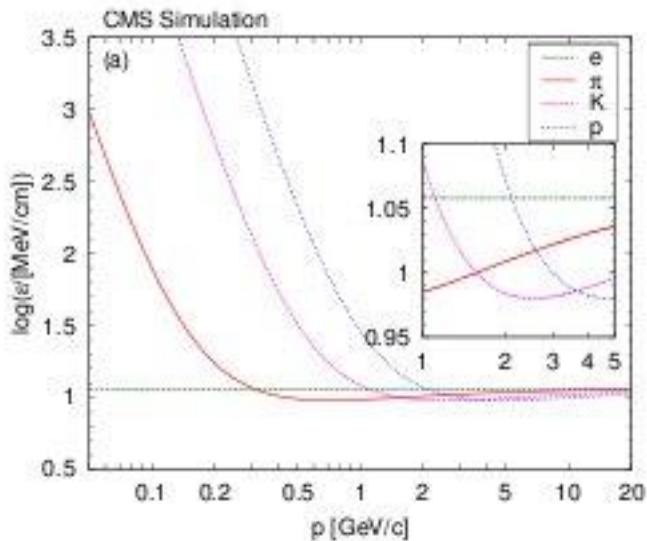


Both T2 NSD enhanced

8 TeV: Triggered by Totem T2

PRL 105(2010) 022002
CMS-PAS-FSQ-12-026
CMS-PAS-QCD-10-024

Identified particle spectra

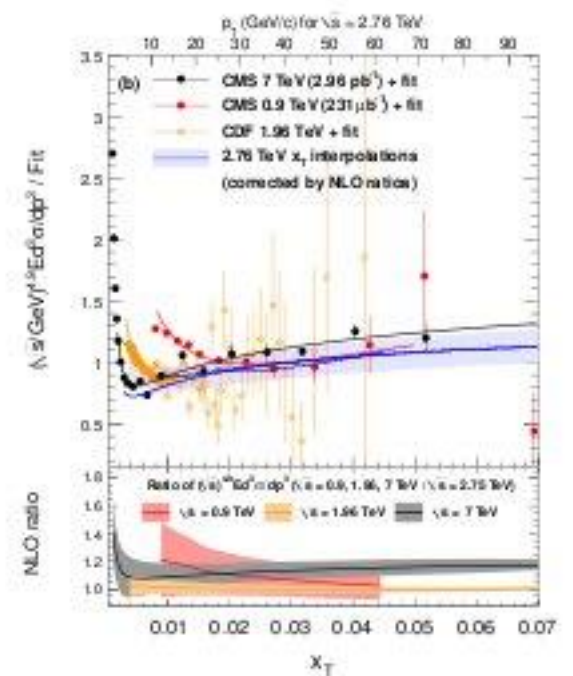
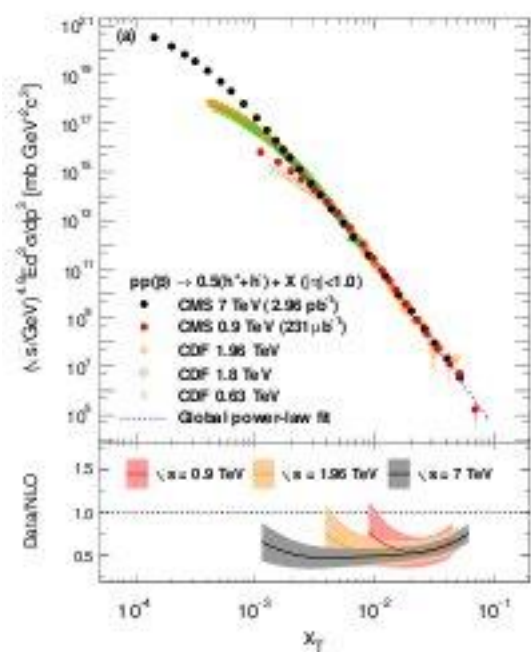
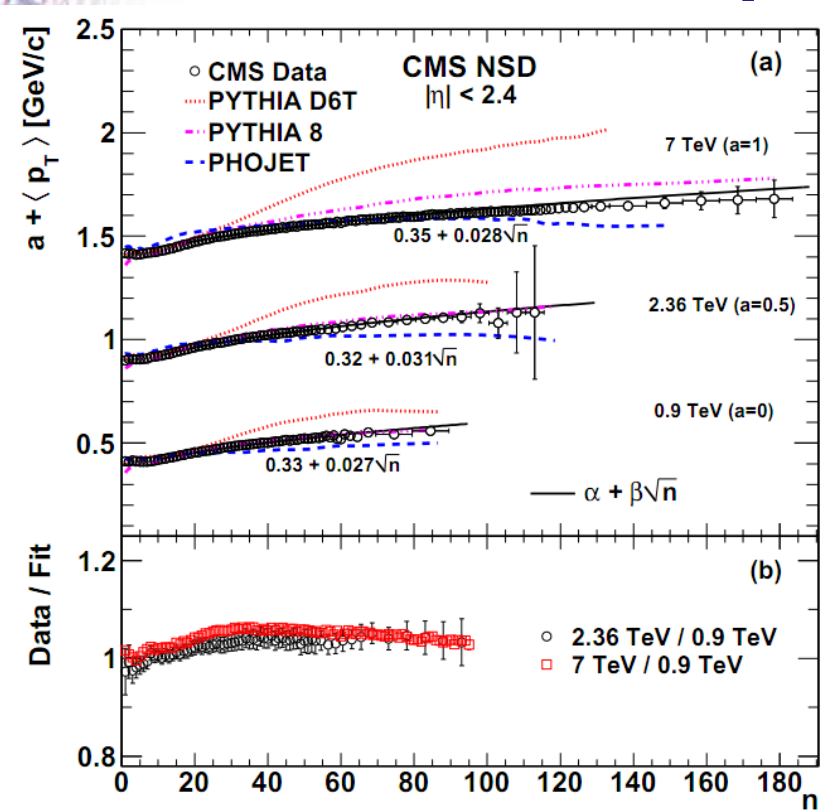


Identified via dE/dx in the silicon layer of the tracker and number of hits per track, track quality in η - p_T bins: combined fit.

Charged hadrons: pions, kaons protons in p_T range 0.1-2 GeV

CMS results consistent with existing results at low \sqrt{s} . Spectra also measured differentially in bins of particle multiplicity, to further constrain hadron production models.

p_T & x_T -Scaling

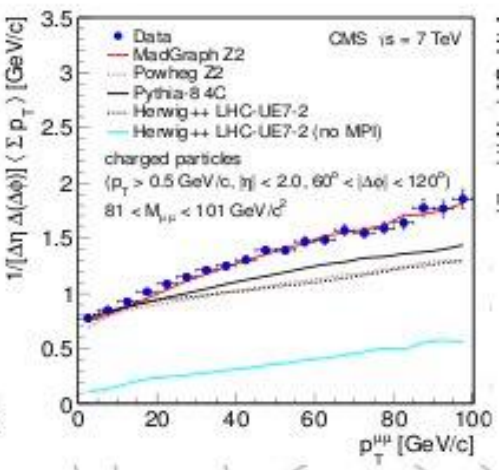
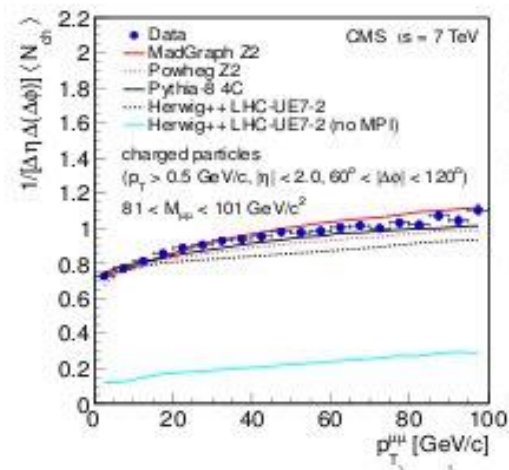
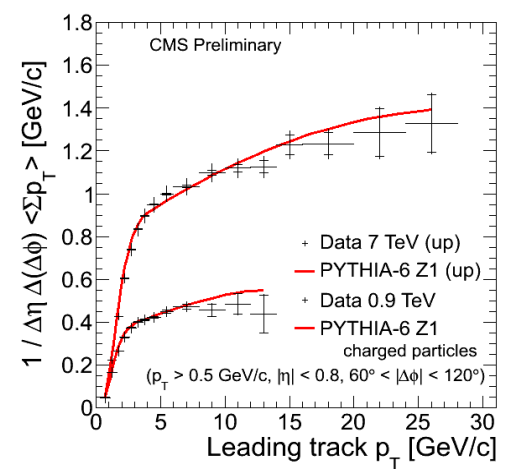
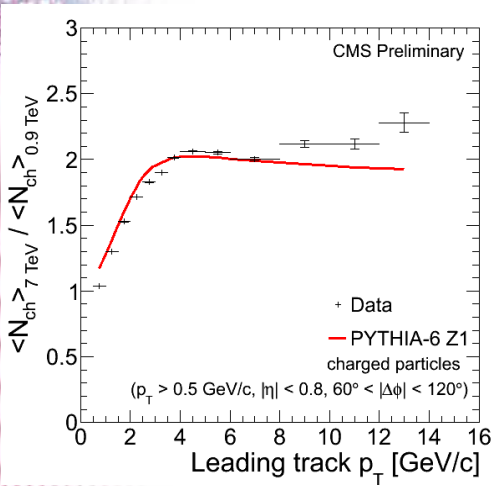


Soft particles:
The rise of the $\langle p_T \rangle$ with multiplicity is energy independent

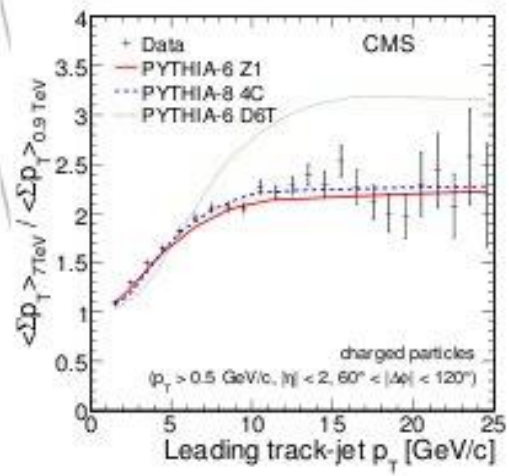
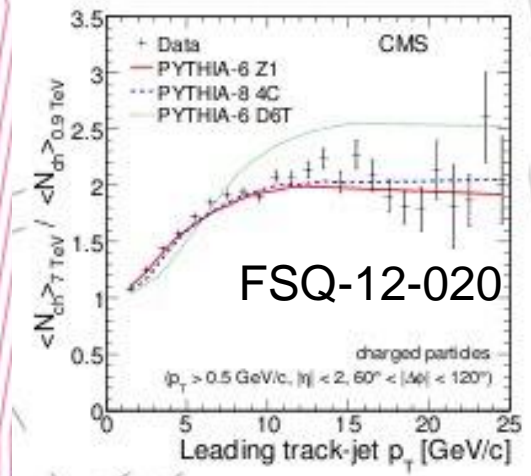
Hard particles:
The CMS results are consistent with $x_T = 2p_T/\sqrt{s}$ scaling (pQCD prediction) with exponent $N = 4.9 \pm 0.1$
NLO calculations overestimates cross-section twice at all energies for high p_T hadrons

Sensitive to the interplay between soft, semi-hard and hard particles production

Underlying event

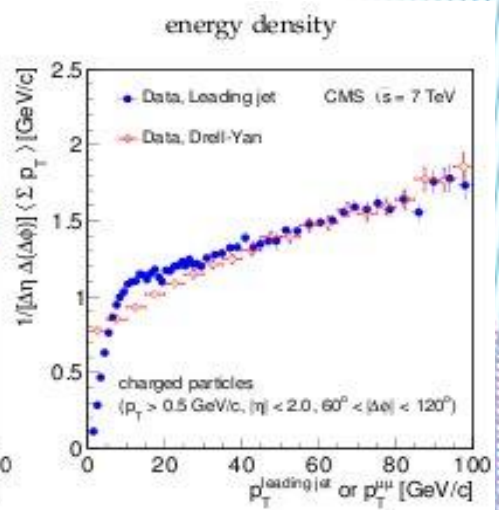
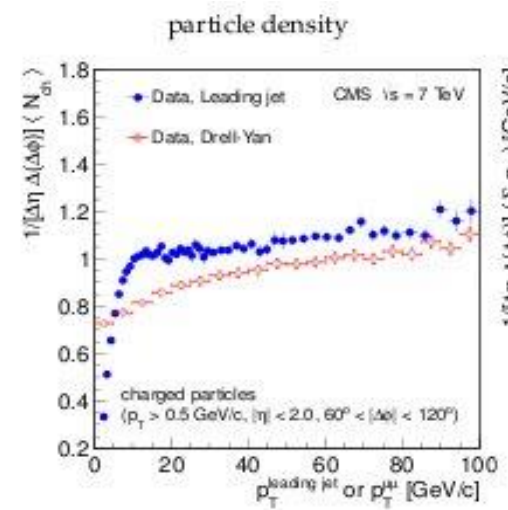


UE in DY events



FSQ-12-020

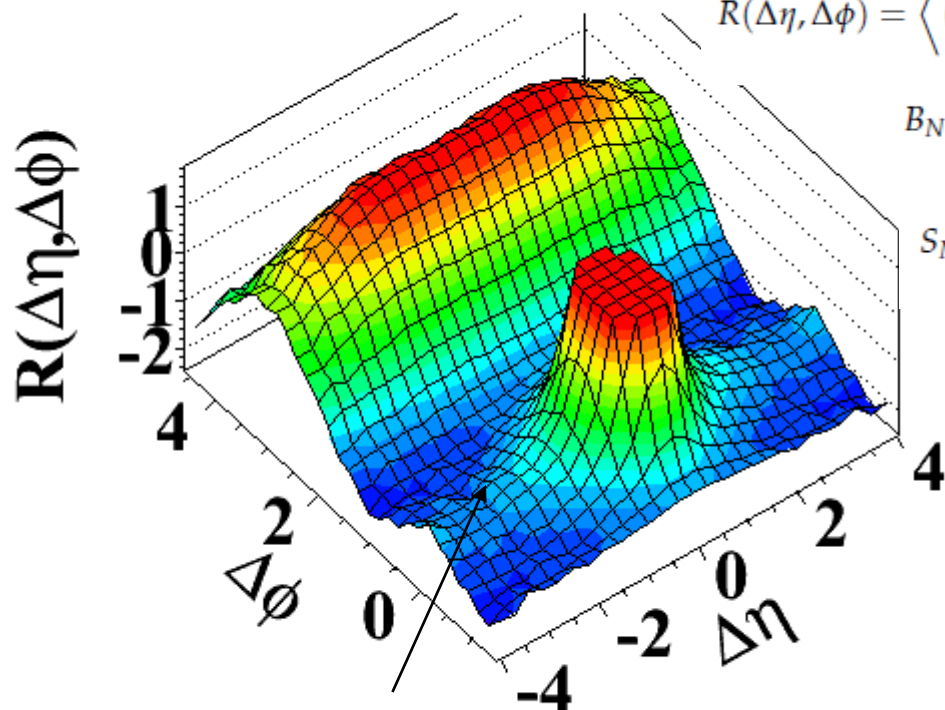
UE in hadronic events with leading track or track jet reflecting the direction of the parton. Sensitive to ISR,FSR,MPI



Comparison of UE in DY w.r.t. Hadronic:

Long range correlations

(d) CMS $N \geq 110$, $1.0 \text{ GeV}/c < p_T < 3.0 \text{ GeV}/c$



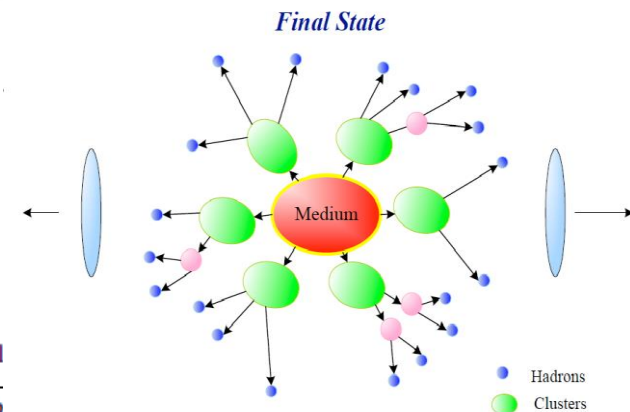
Observation of a LongRange, NearSide angular correlations at high multiplicity in pp events at intermediate p_T (Ridge at $\Delta\phi \sim 0$)

Firstly observed At RICH in Au-Au collisions

$$R(\Delta\eta, \Delta\phi) = \left\langle (N-1) \left(\frac{S_N(\Delta\eta, \Delta\phi)}{B_N(\Delta\eta, \Delta\phi)} - 1 \right) \right\rangle_N$$

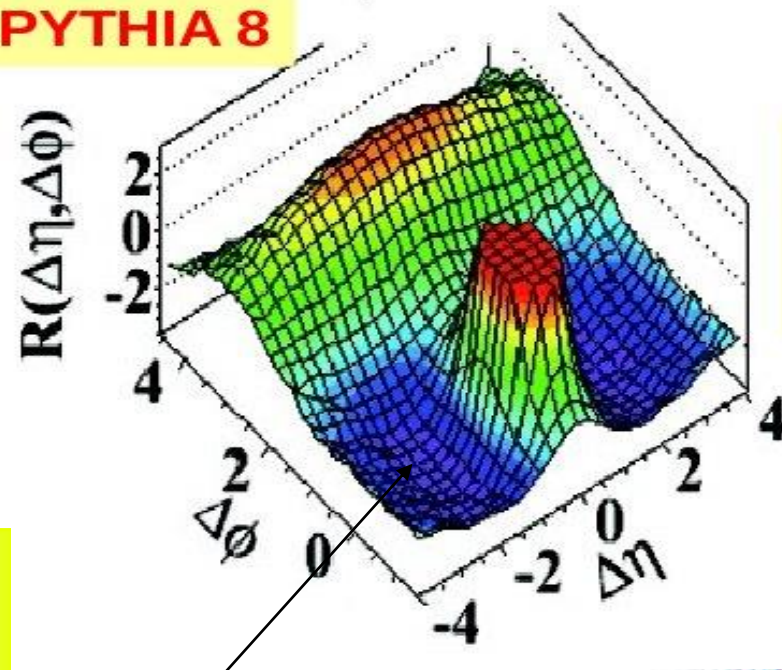
$$B_N(\Delta\eta, \Delta\phi) = \frac{1}{N^2} \frac{d^2 N^{\text{mixed}}}{d\Delta\eta d\Delta\phi}$$

$$S_N(\Delta\eta, \Delta\phi) = \frac{1}{N(N-1)} \frac{d^2 N^{\text{signal}}}{d\Delta\eta d\Delta\phi}$$



(d) $N > 110$, $1.0 \text{ GeV}/c < p_T < 3.0 \text{ GeV}/c$

PYTHIA 8




Ridge is not reproduced neither of PYTHIA versions nor MADGRAPH

Theoretical hypothesis:

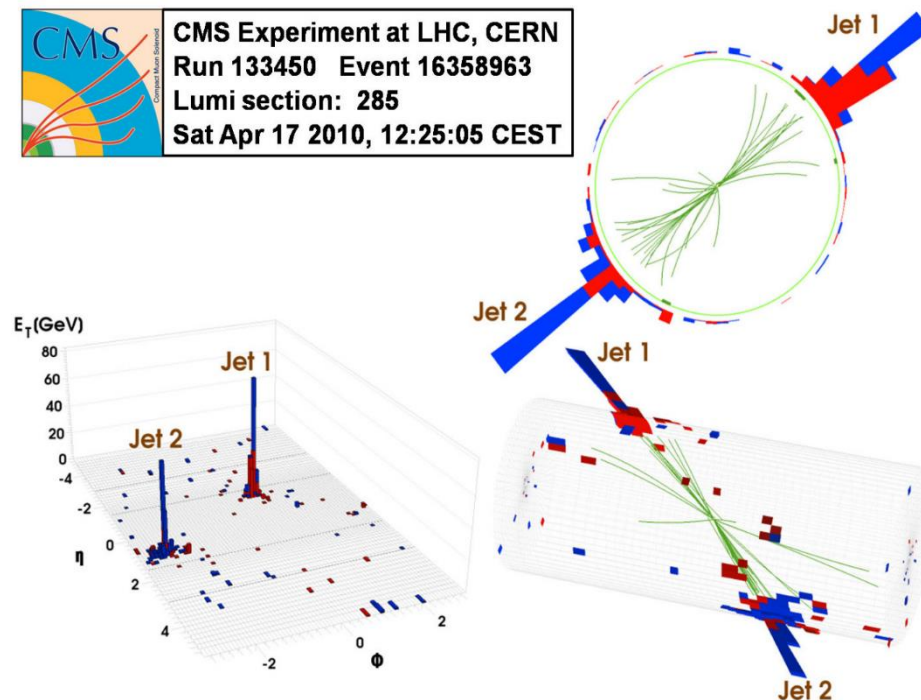
- initial state correlated gluon flow
- collective parton flow effect at the final state

JHEP 1009 (2010) 091

Hard interactions



CMS Experiment at LHC, CERN
Run 133450 Event 16358963
Lumi section: 285
Sat Apr 17 2010, 12:25:05 CEST



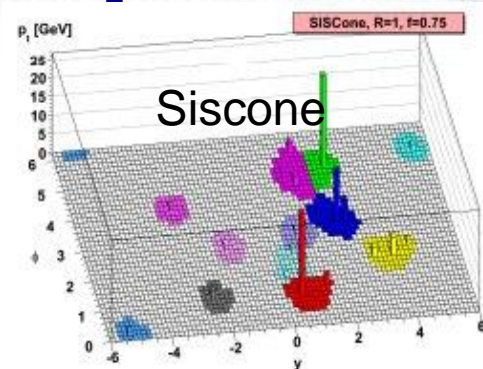
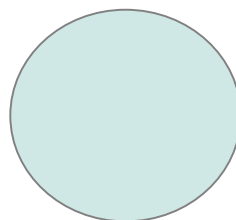
CMS, 7 TeV, 2010 year

Jet clustering techniques

Fixed cone algorithms:

- Iterative Cone (CMS) / JetClu (ATLAS)
- Midpoint algorithm (CDF/D0)
- Seedless Infrared Safe Cone (SISCone)

Iterative cone

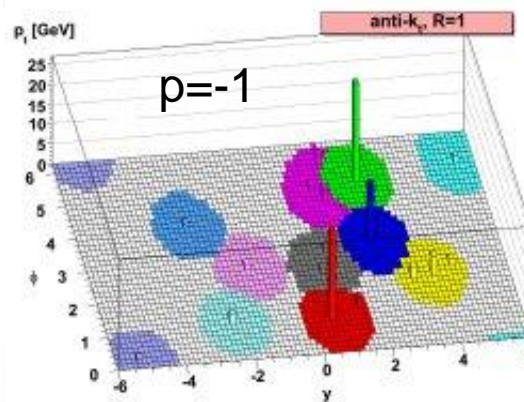
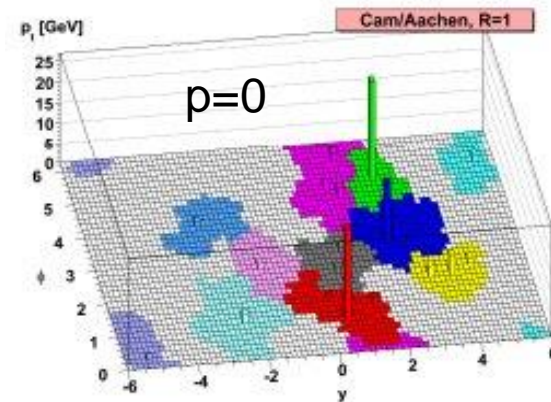
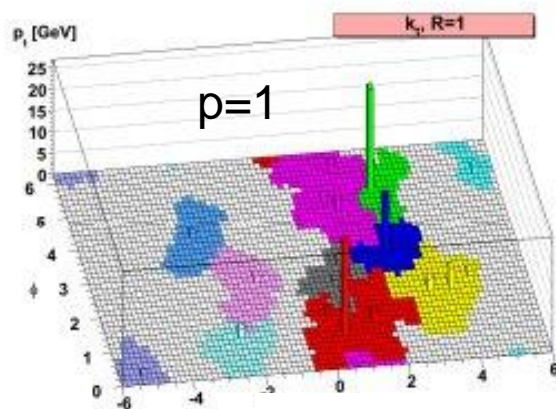


Successive recombination algorithms:

$$d_{ij} = \min(k_{ti}^{2p}, k_{tj}^{2p}) \frac{\delta_{ij}^2}{R^2}$$

$$d_{iB} = k_{ti}^{2p}$$

if ($d_{ij} < d_{iB}$) add i to j
and recalculate p_j



- $p=1$ -> k_T jet algorithm
- $p=0$ -> CA jet algorithm
- $p=-1$ -> "Anti- k_T " jet algorithm

Typical size in η - ϕ space: $0.5 < R < 1$

Jets reconstruction in subdets

Calorimeter jets (CaloJets):

Jet clustered from Calorimeter Towers
 Subdetectors: ECAL, HCAL



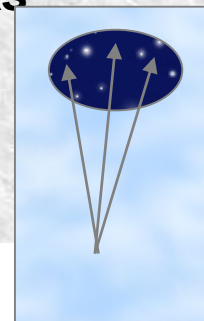
CaloMET

Selected subdetectors participate in reconstruction

Tracker jets:

Jet clustered from Tracks

Subdetectors: Tracker

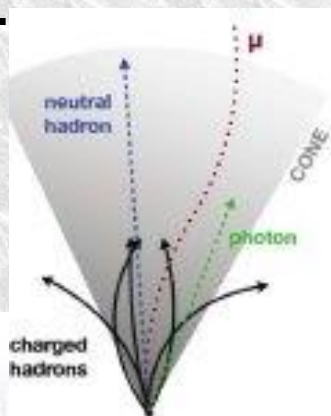


ParticleFlow jets full (PFJets):

Jet clustered from Particle Flow objects (a la generator level particles) which are reconstructed based on cluster separation.

Subdetectors: ECAL, HCAL, Tracker, Muon

PFMET

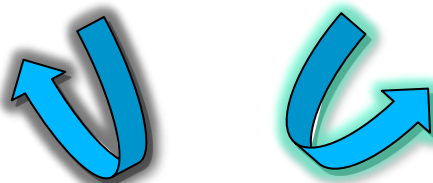


All subdetectors participate in reconstruction:

particle flow reconstruction in two branches

Full

Light



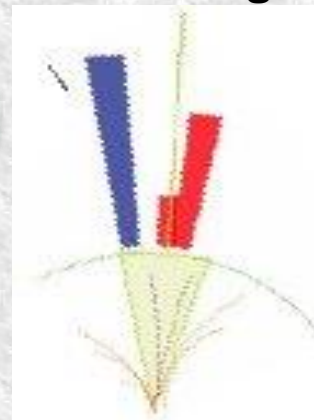
The residual jet energy corrections is applied on top of all algorithms

Particle flow light:

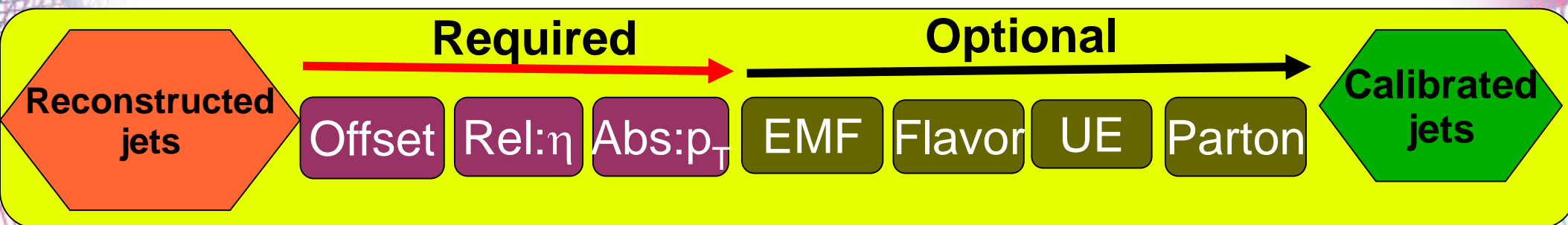
JetPlusTrack jets (JPTJets):

Starting from calorimeter jets tracking information is added via subtracting average response and replacing with tracker measurements.

Subdetectors: ECAL, HCAL, Tracker, Muon
 TcMET



Jet energy corrections schema



Factorized approach for jet energy corrections:

“Offset” - removes unwanted contribution from noise and pileup

“Relative” - removes variation of response vs η w.r.t the central region (in-situ: dijet p_T balance)

“Absolute” - removes variation of jet response vs jet p_T (in situ: Photon+jet p_T balance, MPF method)

“Residual” - remove the residual difference between JES in MC and Data

Two sources of the correction:
 Monte-Carlo simulations
 In-situ measurements with physics process

We correct for:

Calorimeter response

Magnetic field

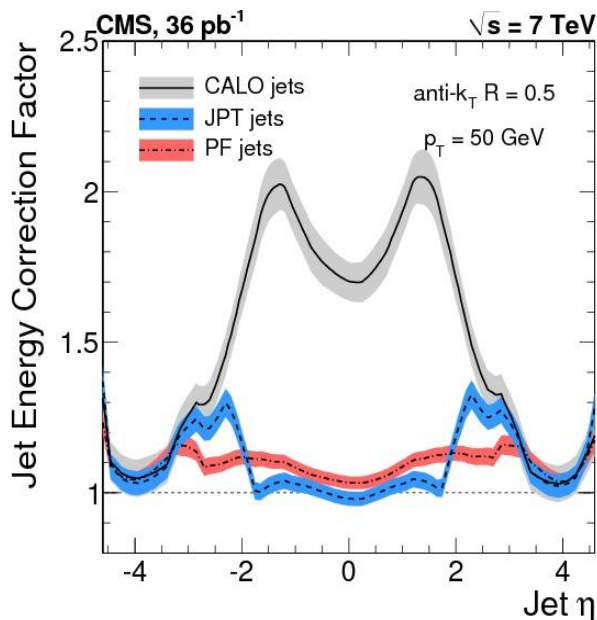
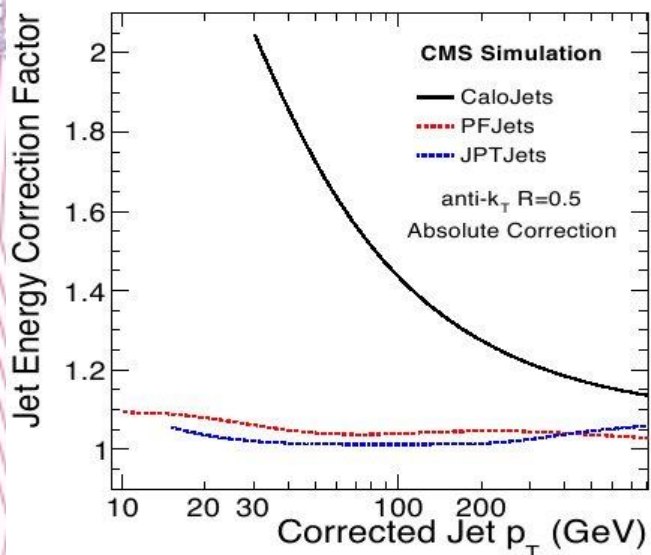
Electronic noise/tower thresholds

Dead materials and cracks

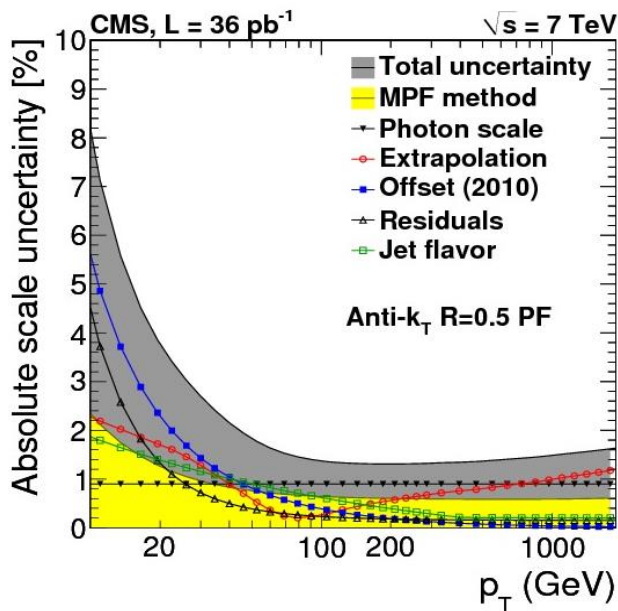
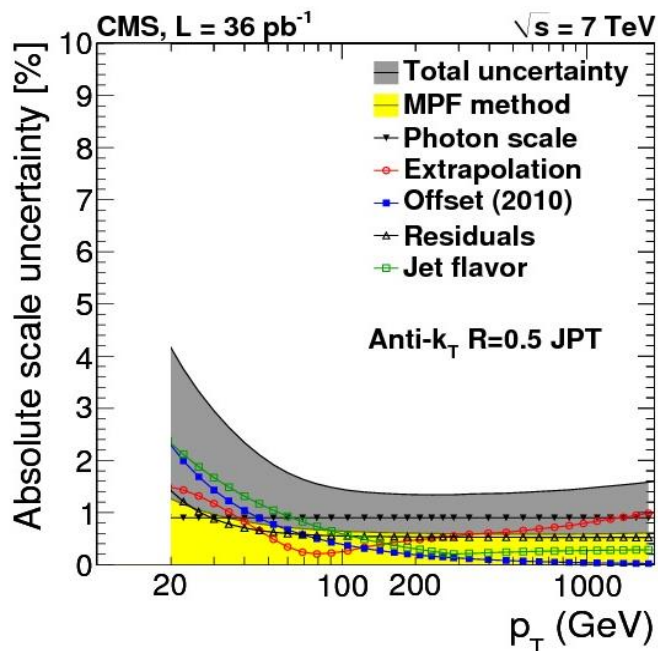
Longitudinal leakage

Shower size, out of cone loss

Jet performance



use of tracker detectors decreases the value of the residual corrections.



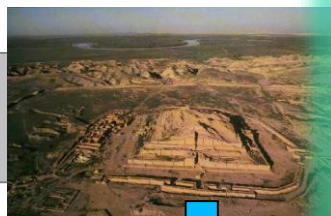
The better we know response function the more exact measurements deconvolution we can perform

Two notes towards jet production measurement

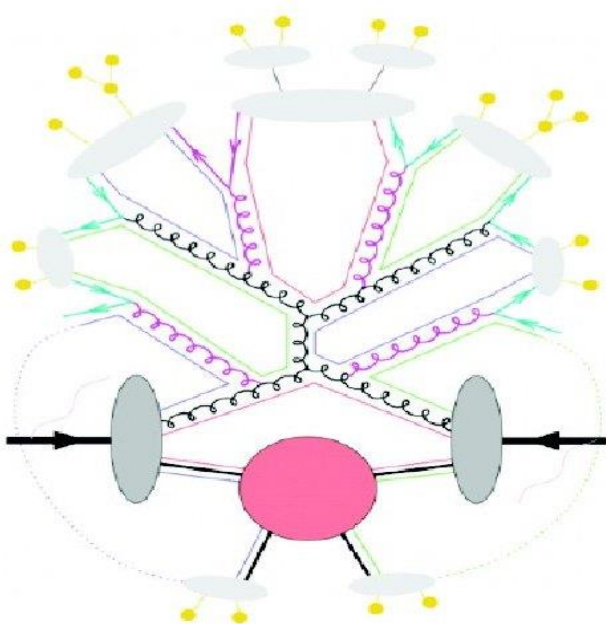
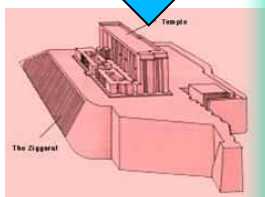
Measurements

Measurements are corrected to particle level via either unfolding procedure or bin-to-bin corrections

Detector vision

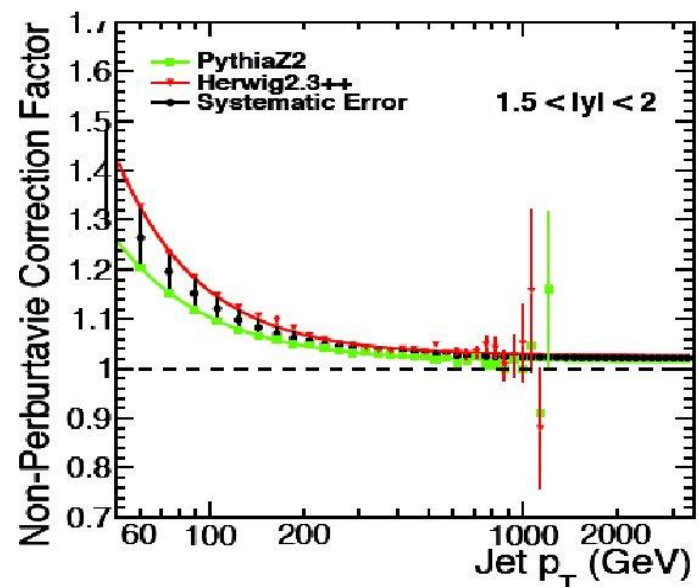


Unfolding



Theory

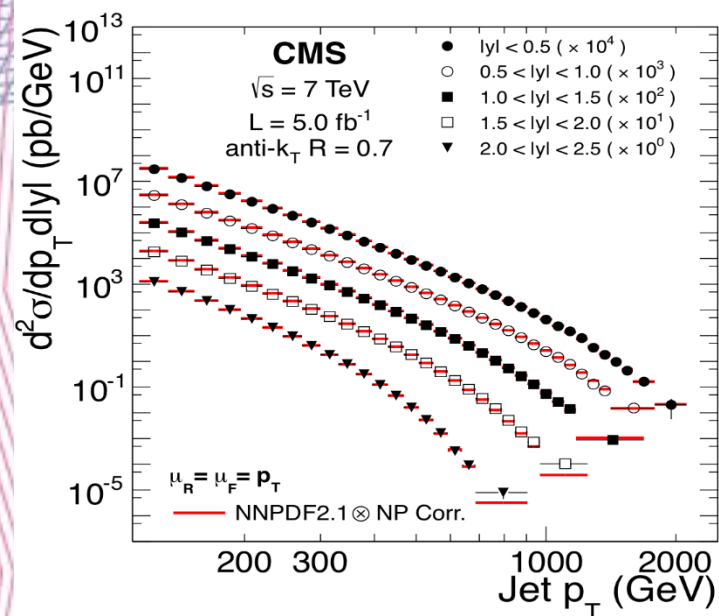
NLO calculations are corrected to particle level for fragmentation and MPI effect with and without Including parton showering using **LO+PS generators**



PDFs parametrization depends on the choice of the input data, order of pQCD, heavy Qs treatment, correlations between PDFs and α_S , treatment of uncertainties

Inclusive central jets production

Jets: $|\eta| < 2.5$



Motivation: constrain PDFs, differentiate between the different PDF sets: CT10, HERA1.5, MSTW2008, ABKM09

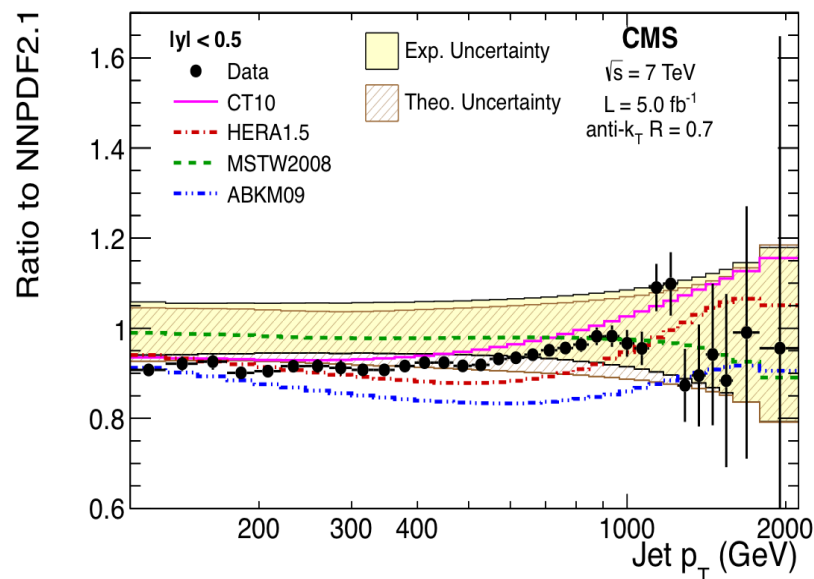
7 TeV

Measured jet p_T spectra in 5 rapidity bins were unfolded to particle level jet spectra using dAgostini Multidimensional unfolding method.

NLO calculations with non-perturbative (NP) corrections are used for comparison with data. NP corrections are got as averaged value estimated with PYTHIA and HERWIG.

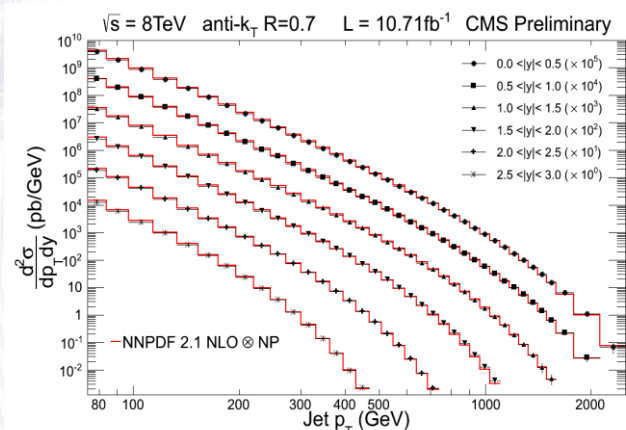
A set of the different NLO PDFs is used to account for PDF uncertainty.

Data are in agreement with NLO calculations within systematic uncertainties although NLO calculations are systematically overestimate cross-section in all rapidity bins.





Inclusive central jets production



PDF sets considered: **ABM11**, **HERA1.5**, **CT10**, **MSTW2008**, **NNPDF2.1**

Jets: $|\eta| < 3$

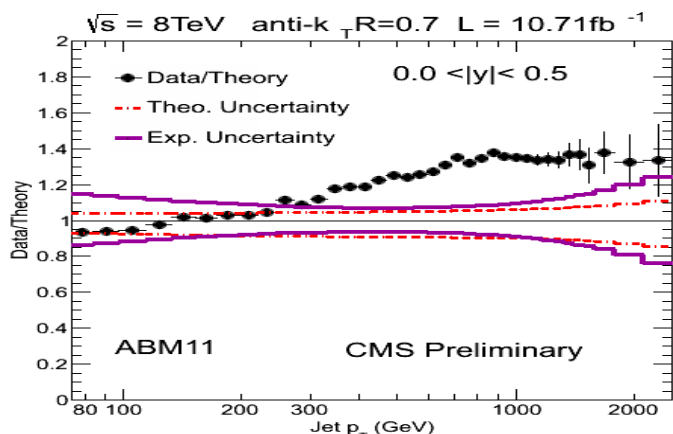
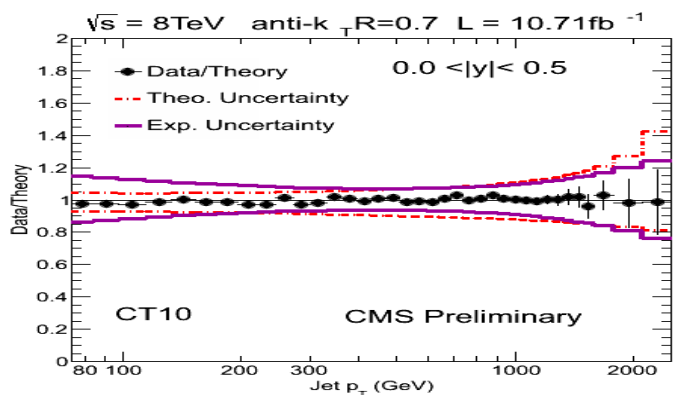
The total experimental uncertainty gets contribution from JES(12%-30%)
Luminosity(4.4%)
Unfolding(1%-10%)

8 TeV

resulting into 15%-40% total relative experimental uncertainty on the measured cross-section.

The total theory uncertainty gets contribution from PDF(5%-30%)
Scale(5%-40%).

PDF uncertainty for CT10 in outer bins 100%



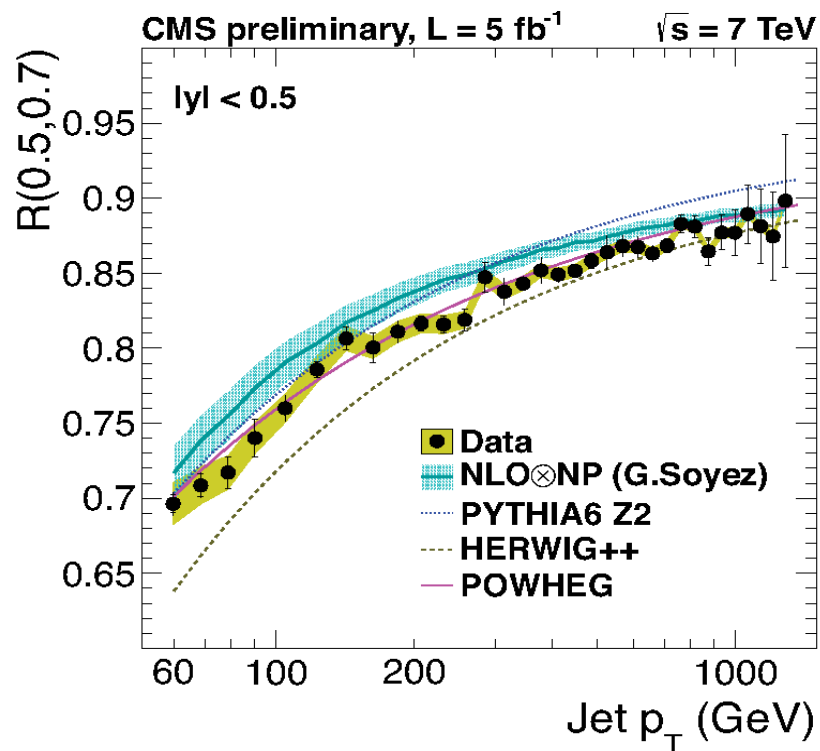
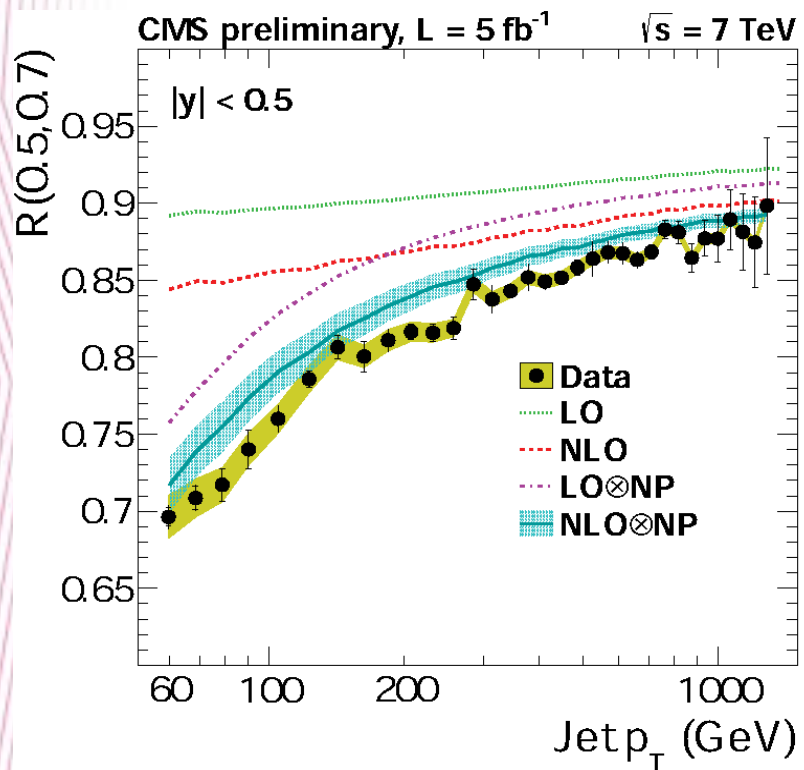
The tested parton momentum fraction is $0.019 < x < 0.625$

Data are in agreement with NLO calculations within systematic uncertainties for all considered PDFs sets except ABM11 PDF set

CMS-PAS-SMP-12-012

Inclusive Jet AK5/AK7 Cross-section ratio

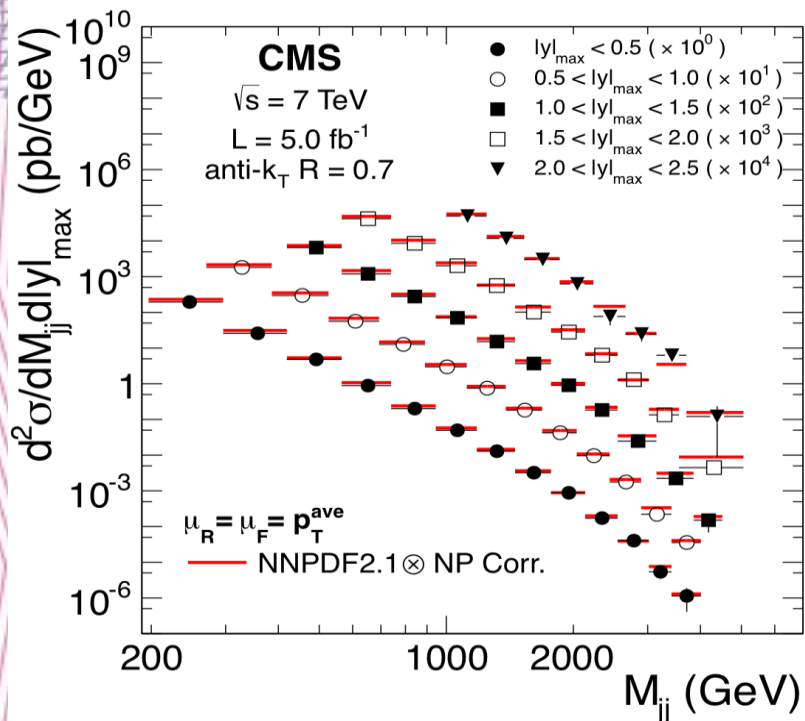
Measurement at 7 TeV with different jet sizes $R=0.5$ (AK5), 0.7 (AK7)
 Ratio of cross sections $R(0.5, 0.7)$ vs p_T and rapidity



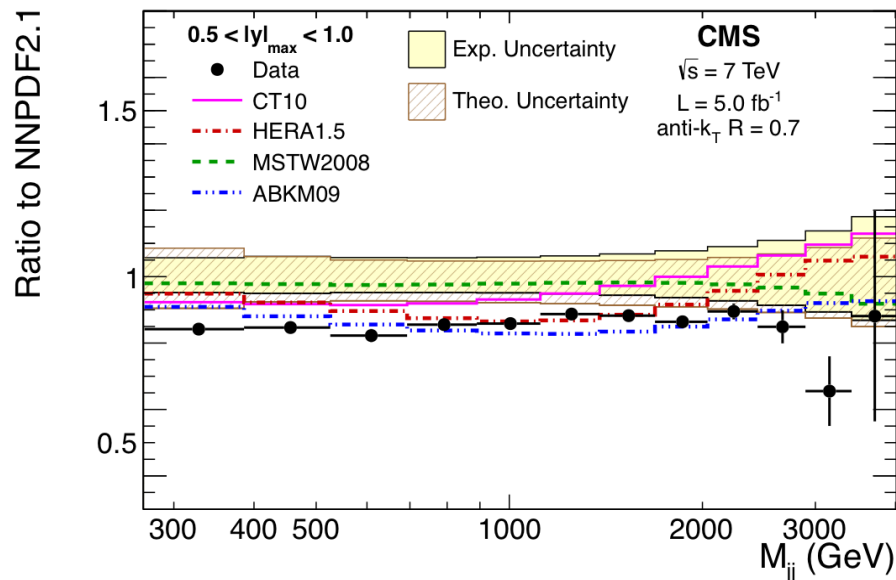
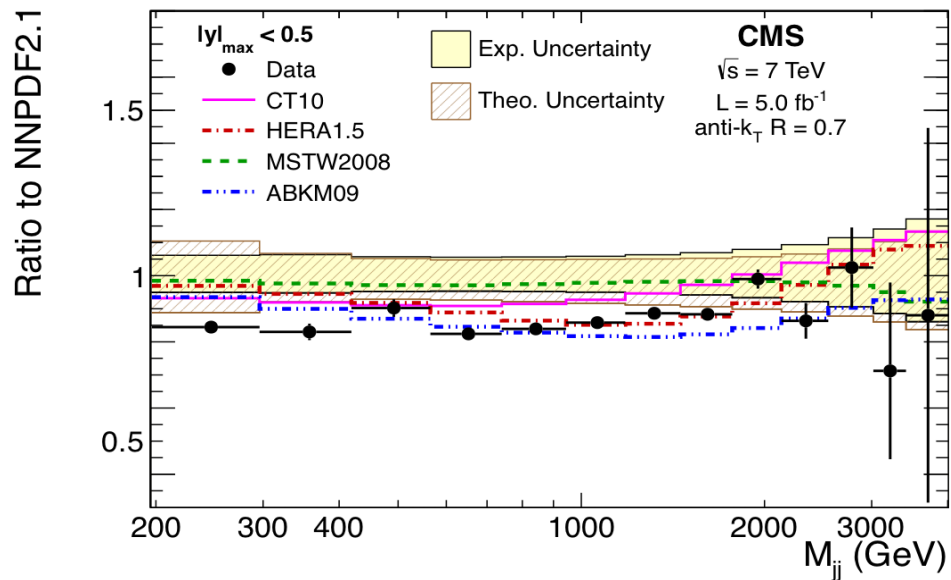
Several systematic uncertainties cancel in ratio
 The ratio gradually increases towards unity with increasing Jet- p_T
 Powheg(NLO+PS) prediction has the describes the data best

CMS-PAS-SMP-13-002

Dijet production



7 TeV



NLO QCD (NLOJet++) + NP corrections

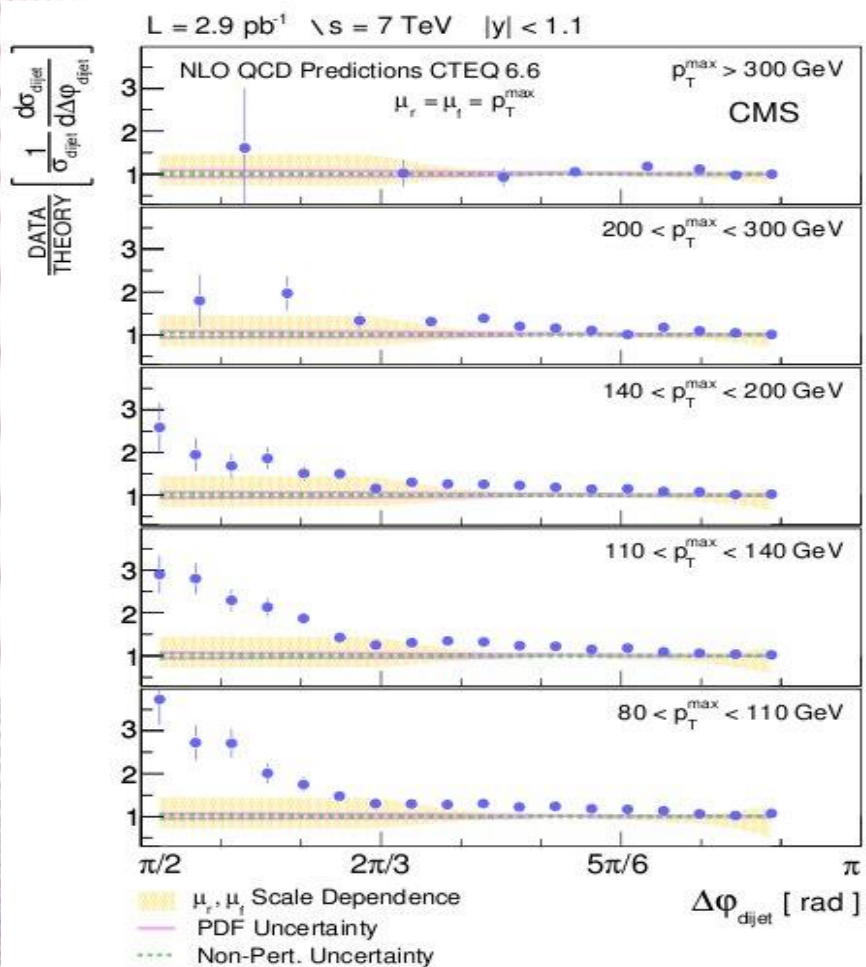
Comparisons with data are done for the different PDFs in the different rapidity bins.

Consistent with NLO calculations within uncertainties, gives the constraint to PDFs.

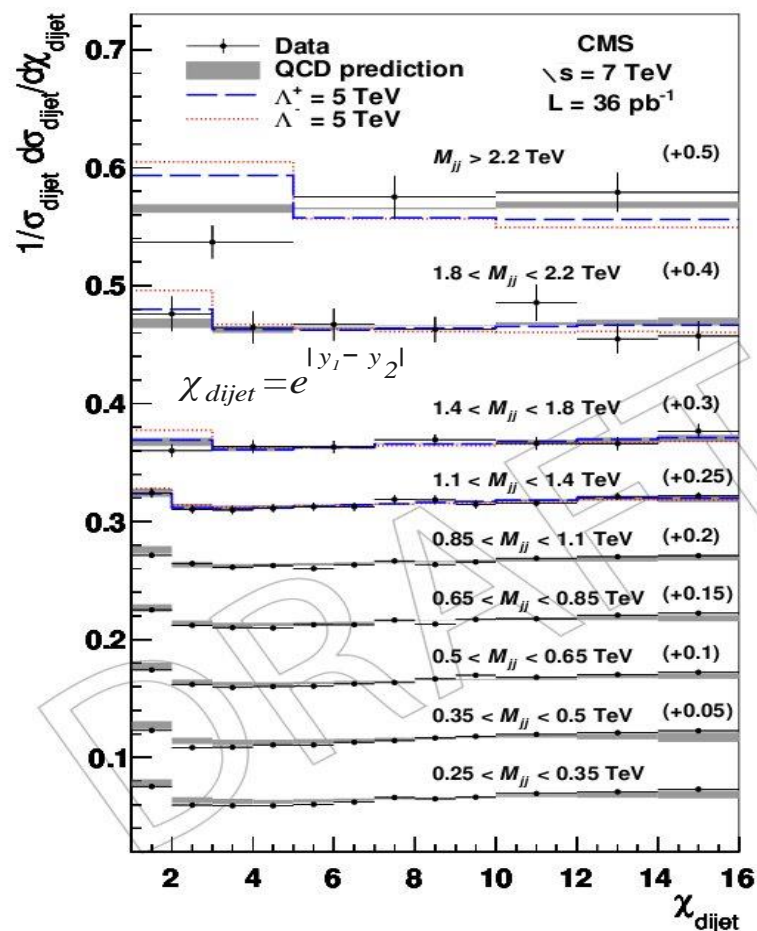
Dijet production: $\Delta\phi, \Delta\eta$

Sensitivity to the initial and final state radiation.

NLO QCD (NLOJet++) + NP corrections disagree with data at small $\Delta\phi$ where multiparton radiation effects dominate.



Good agreement of the dijet angular distribution with NLO QCD + NP corrections. A lower limit on the contact interaction scale 5.6 TeV(+), 6.7 TeV(-) is obtained.

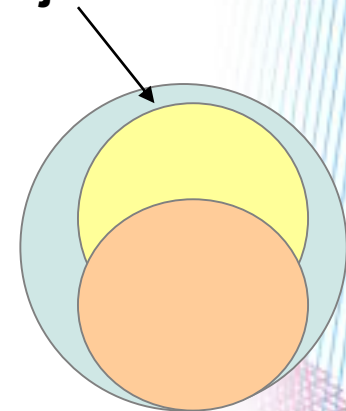


Dijet Mass and Jet substructure

Differential distributions in jet mass for inclusive dijet events, defined through the anti- k_T algorithm for a size parameter of 0.7 for jets groomed through filtering, trimming, and pruning.

Benchmark for them
Massive particles search:

W, Z, massive particles are produced with large boost resulting in “massive” jet



After initial clustering

Filtering:

recluster jet with CA with $R=0.3$, take the 3 highest subjets, re-estimate the 4-vector of jet from 3 subjets

Trimming:

Ignores particles falling below dynamic threshold

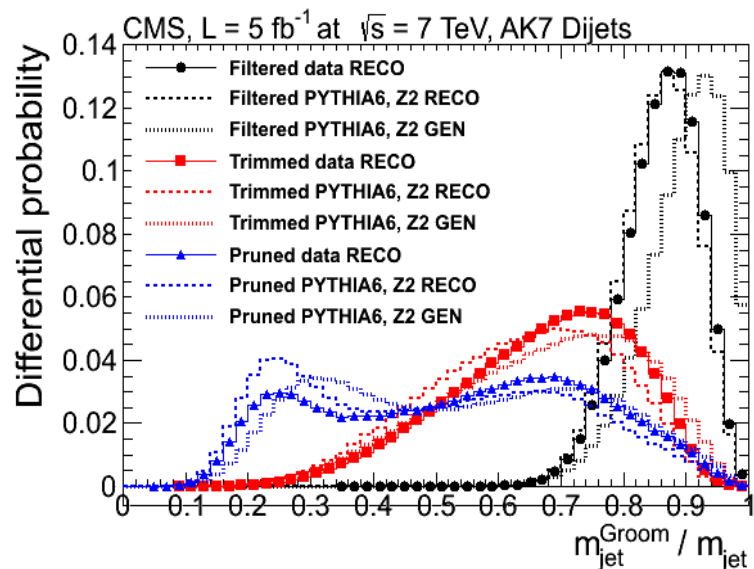
Recluster with k_T with R_{sub} (0.2) and keep subjets with $p_{T sub} > f_{cut} \times \lambda_{hard}$; $f_{cut} = 0.03$

Pruning:

Recluster jet with CA, using the same distance as initial algo but with additional parameters

JHEP05(2013)090

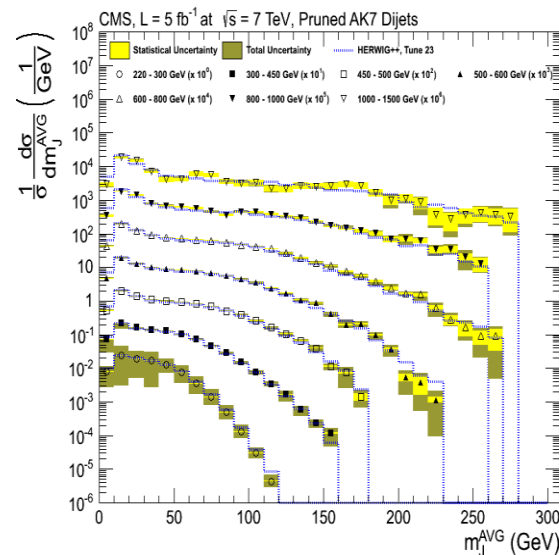
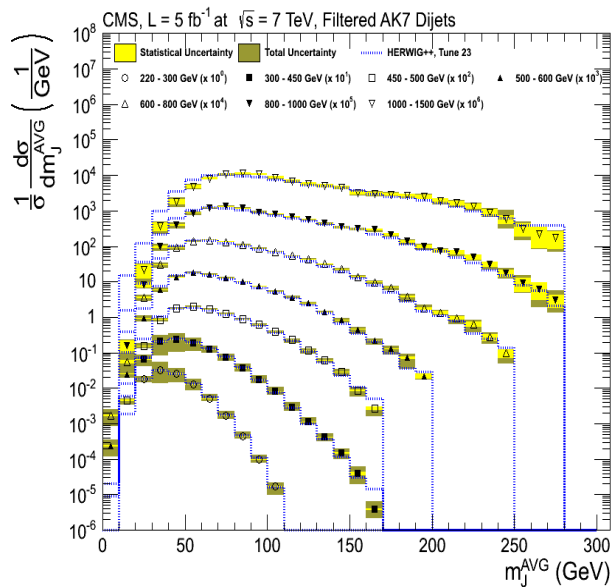
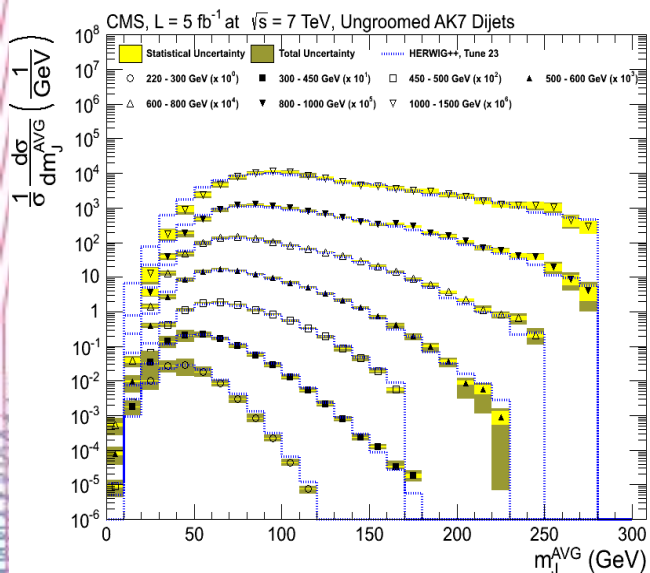
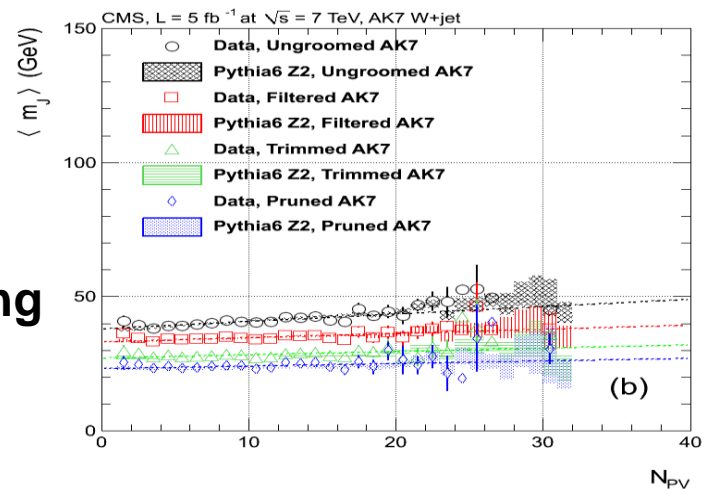
Dijet Mass and Jet substructure

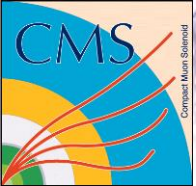


Pruning algorithm
Is the most aggressive

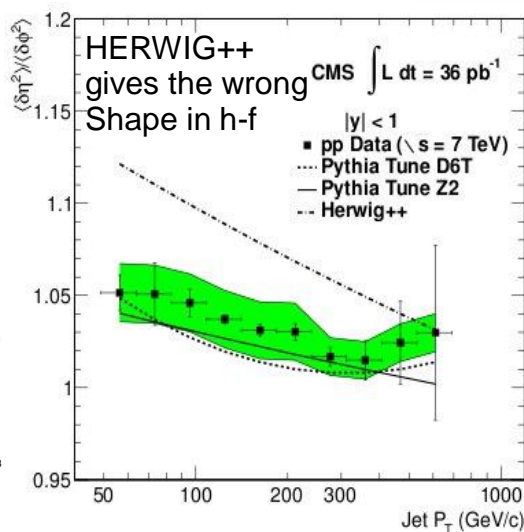
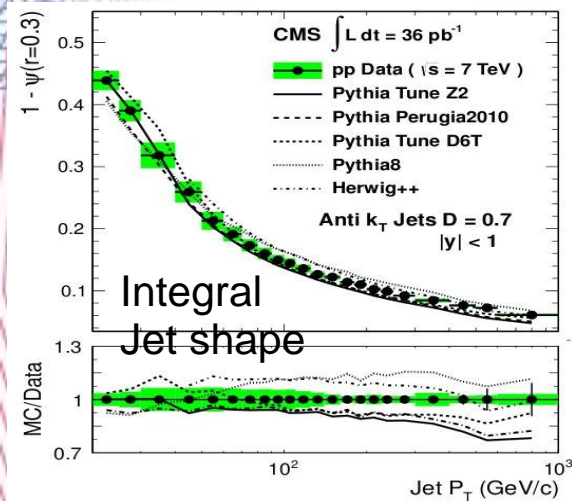
Groomed jets are stable
w.r.t pileup – favorize the use
With high-lumi runs

important benchmark
for use of the grooming
algos in searches
for massive particles.





Jets properties: charged particles multiplicity, shape



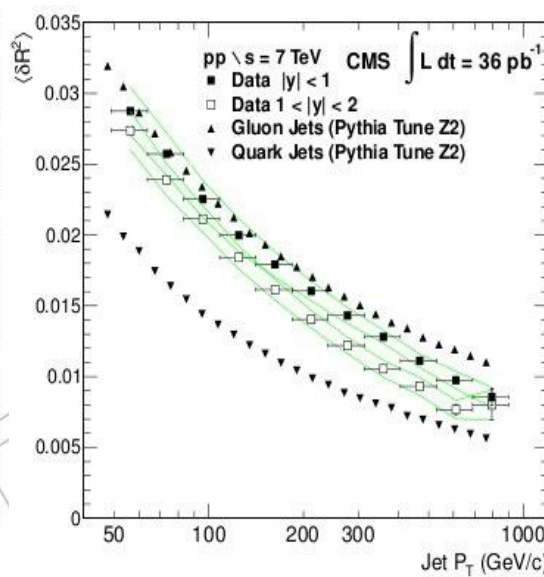
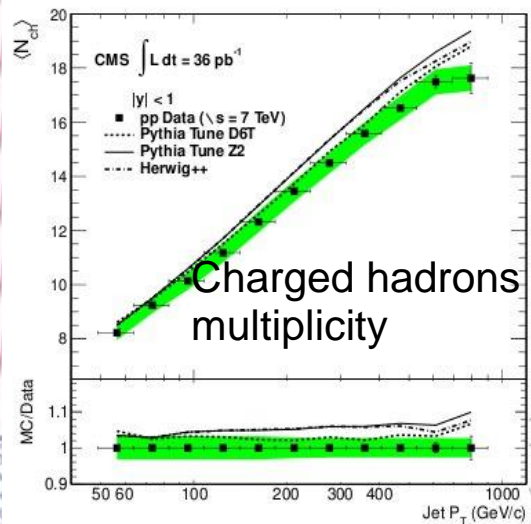
$$\langle \delta R_2 \rangle(p_T) = \langle \delta \phi_2 \rangle(p_T) + \langle \delta \eta_2 \rangle(p_T)$$

$$\langle \delta X_{jet}^2 \rangle(p_T) = \frac{\sum_{i \in jet} (X_i - \langle X \rangle)^2 \cdot p_{Ti}}{\sum_{i \in jet} p_{Ti}} \quad X = \eta \text{ or } \phi$$

Unfolding to particle jets is done with bin-to-bin and Tikhonov regularization method with the quasi-optimal solution.

Jets become narrower with increasing p_T and $|y|$

Agreement with predicted increase in the fraction of quark-induced jets at higher jet p_T and $|y|$



Results gives impact to modeling PDFs, parton showering, fragmentation function



Multijet production (3 jets)

Measurement of double differential cross section:

$$d^2\sigma/dm_3 dy_{\max}$$

sensitivity to PDFs and α_s

$$m_3^2 = (p_1+p_2+p_3)^2, |y_{\max}| = \max(|y_1|, |y_2|, |y_3|), Q = m_3/2$$

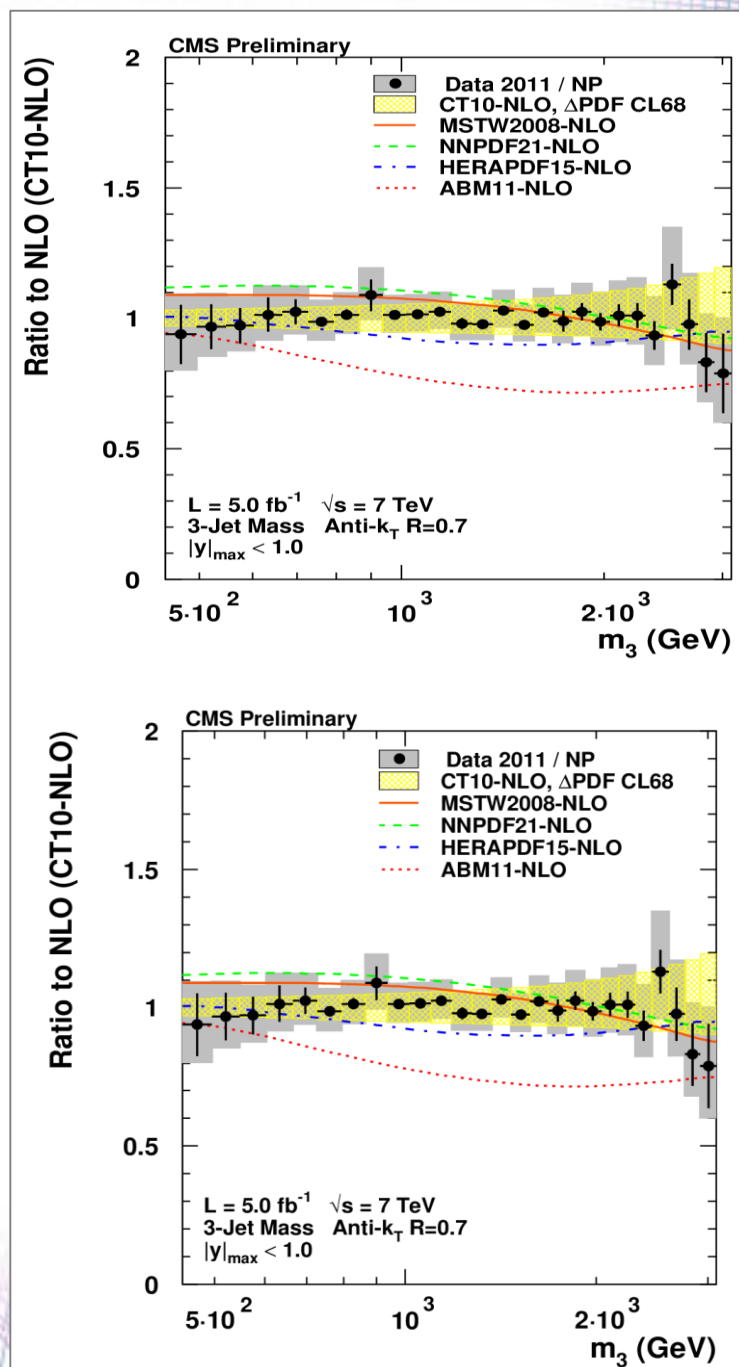
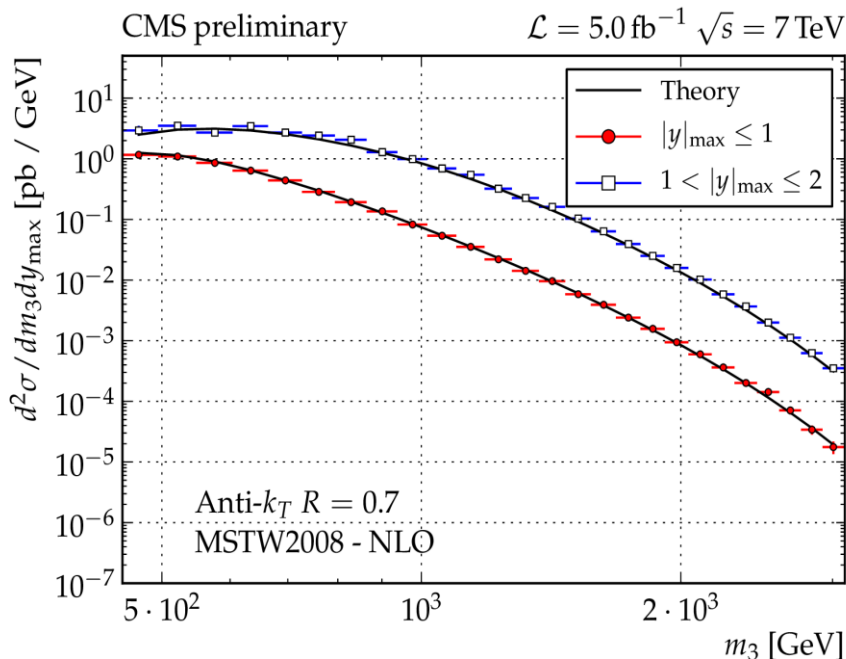
Require jet $p_T > 100$ GeV

Regions: $|y_{\max}| < 1$ and $1 < |y_{\max}| < 2$ - reach up to $m_3 \sim 3$ TeV

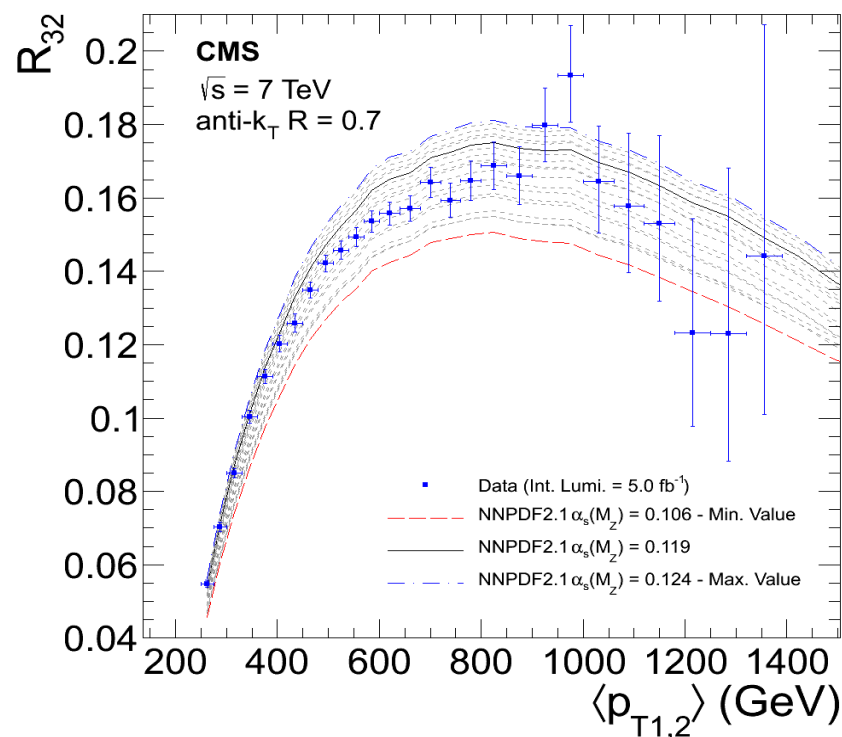
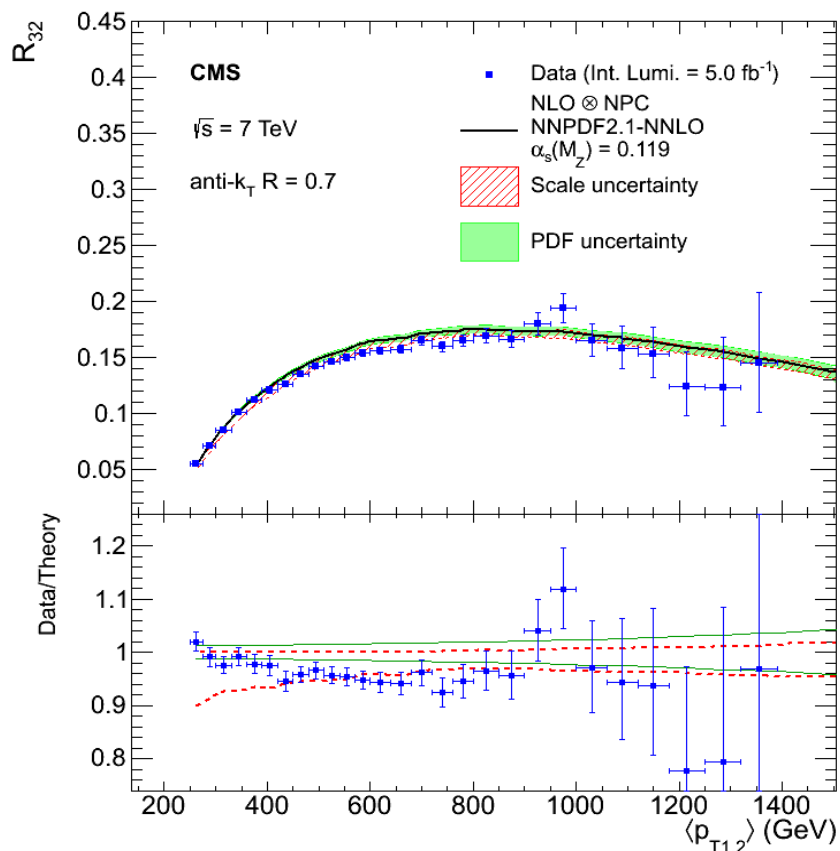
Agreement with pQCD @ NLOxNP

(NP correction 8% \rightarrow 1%)

Deviations observed with NLO + ABM11 PDF



3-jet over 2-jet cross section ratio



$$R_{32} = \sigma(n_{\text{jet}} \geq 3) / \sigma(n_{\text{jet}} \geq 2)$$

Cross-section ratio R32:

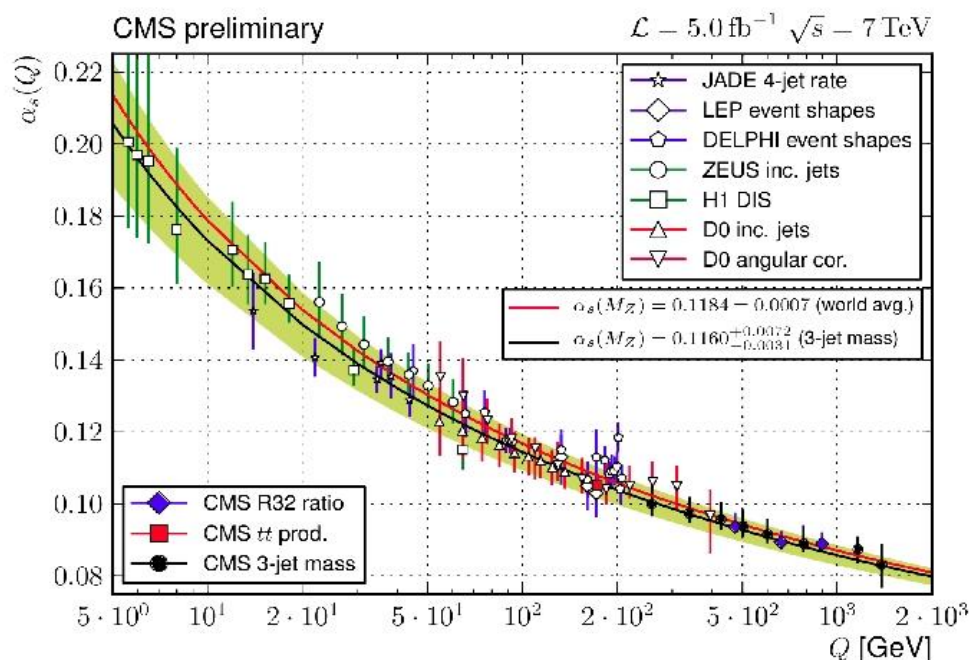
- inclusive 3-jet over 2-jet production
- sensitive to α_s

Multiple alternative phase-space options

- depending on the cut imposed on the 3rd jet p_T
- measuring the α_s : vital to reduce scale uncertainty

$\alpha_s(M_Z)$ extraction from 3-jet events

1. From the ratio of the 3 jets/2 jets cross-sections
2. Fit of the data to theory predictions in 8 regions of the 3-jets mass using MSTW2008-NLO PDF set and NLO evolution order from Eur. Phys. J. C 5 (1998) 461



CMS-PAS-QCD-11-003
CMS-PAS-SMP-12-027

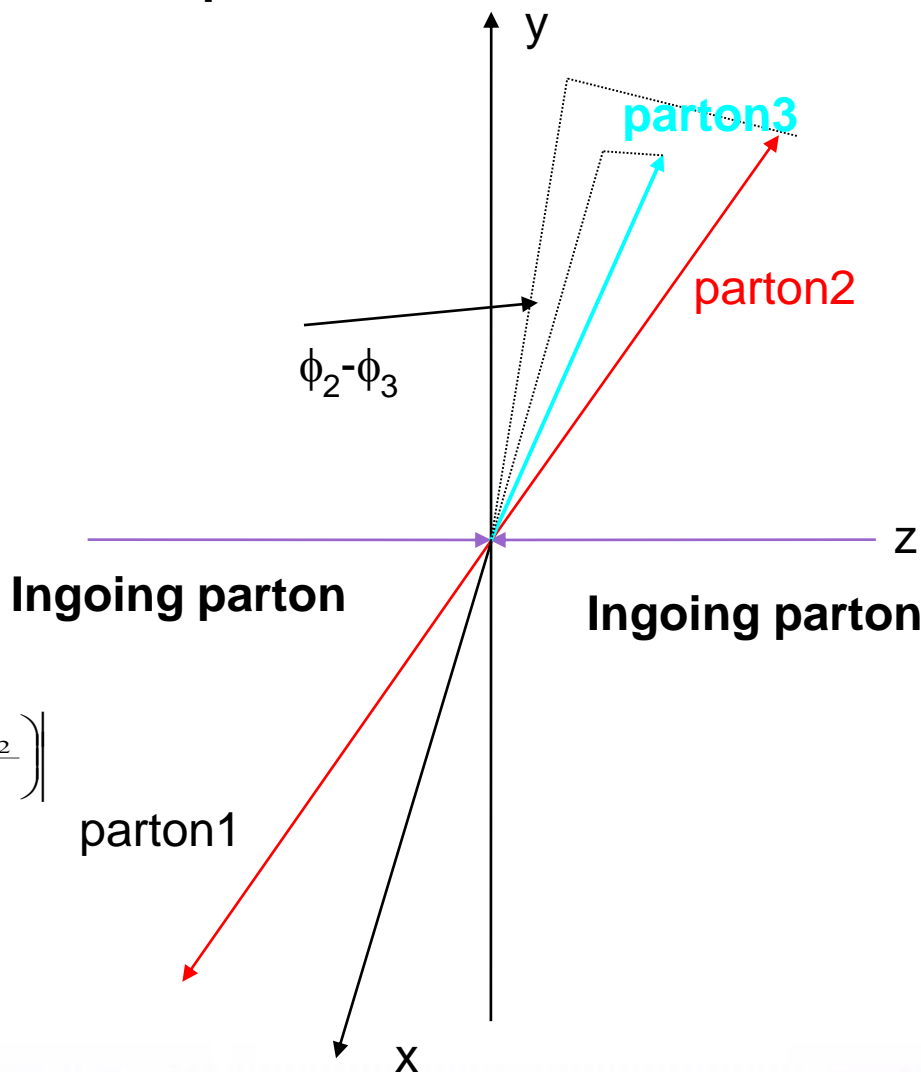
- Results are comparable with world average $\alpha_s(M_Z) = 0.1184 \pm 0.0007$
- For the first time probing the $> 1 \text{ TeV}$ scale, reaching up to $\sim 1.4 \text{ TeV}$
- Dominated by theoretical uncertainties (PDF and scale)

R₃₂: $\alpha_s(M_Z) = 0.1148 \pm 0.0014$ (exp.) ± 0.0018 (PDF) $+0.0050 -0.0000$ (scale)

3-jet mass: $\alpha_s(M_Z) = 0.1160^{+0.0025}_{-0.0023}$ (exp, PDF, NP) $+0.0068 -0.0021$ (scale)

Color coherence

Outgoing partons produced in the hard interaction continue to interfere with each other during their fragmentation phase.



In the presence of the color coherence third parton tends to be in the plane defined by beam and the second parton e.g. $\beta \rightarrow 0$ or $\beta \rightarrow \pi$

In the absence of the color coherence there is no preferred direction in the emission of the third parton around radiating parton

Observable:

$$\beta = \left| \arctan \left(\frac{\varphi_3 - \varphi_2}{\eta_3 - \eta_2} \right) \right|$$

parton1

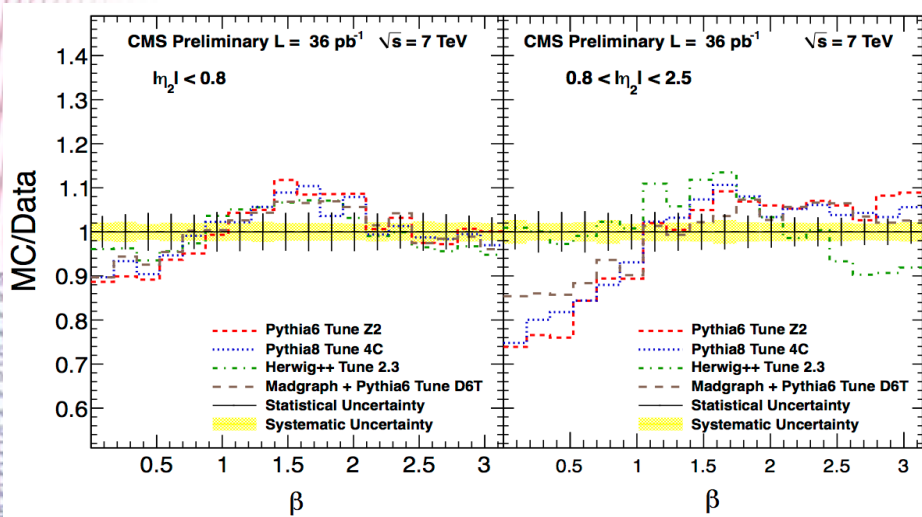
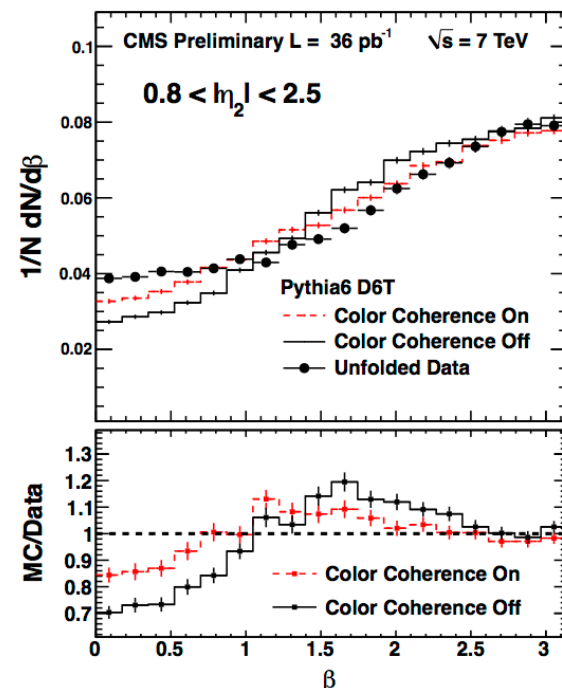
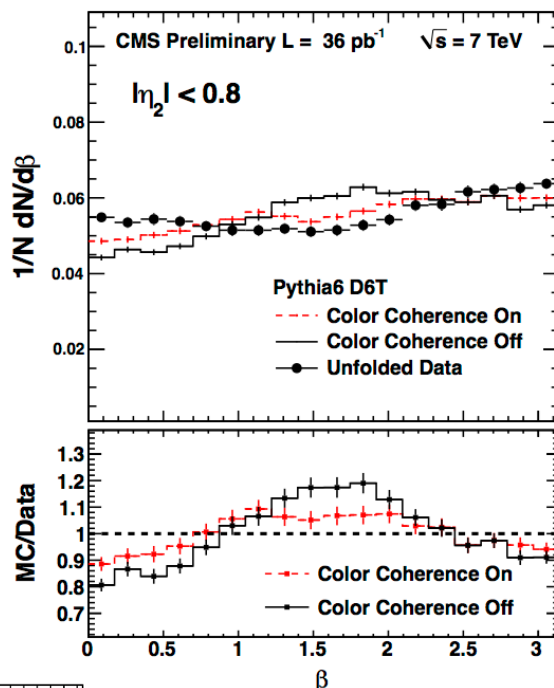
CMS-PAS-SMP-12-010

Color coherence

Analysis of the color coherence was done with 3 jet events:

$p_{T1} > p_{T2} > p_{T3}$
 $|\phi_1 - \phi_2| > 2.7$ (back-to-back)
 $P_{T1} > 100$ GeV
 $P_{T2} > 30$ GeV
 $M_{12} > 220$ GeV
 $0.5 < \Delta R_{23} < 1.5$

7 TeV, 36 pb⁻¹



β is sensitive to the color coherence effect

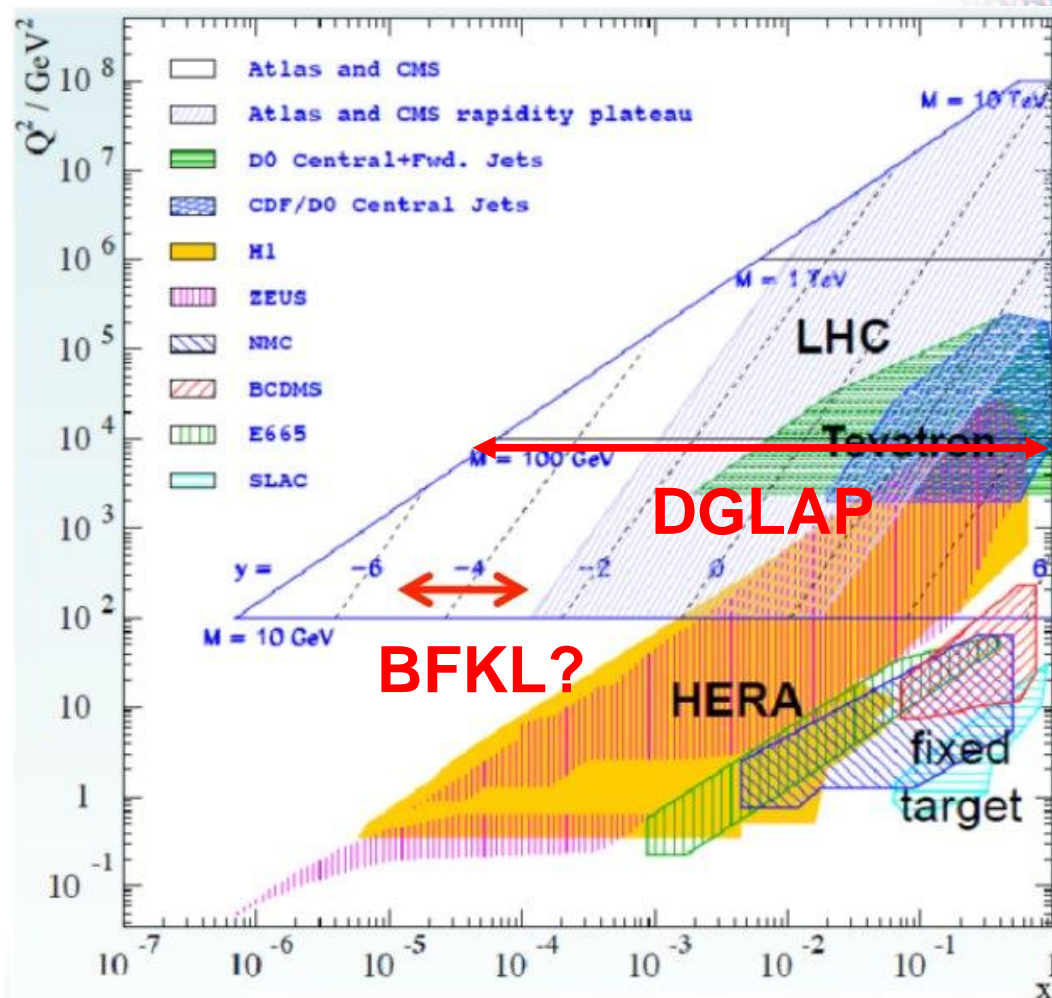
Considered MC models have the implementation Of the color coherence but none of them is fully successful

Small-x QCD

Connection between various scales in QCD (for instance, between PDF and the high-momentum scattering) is performed via evolution differential equations.

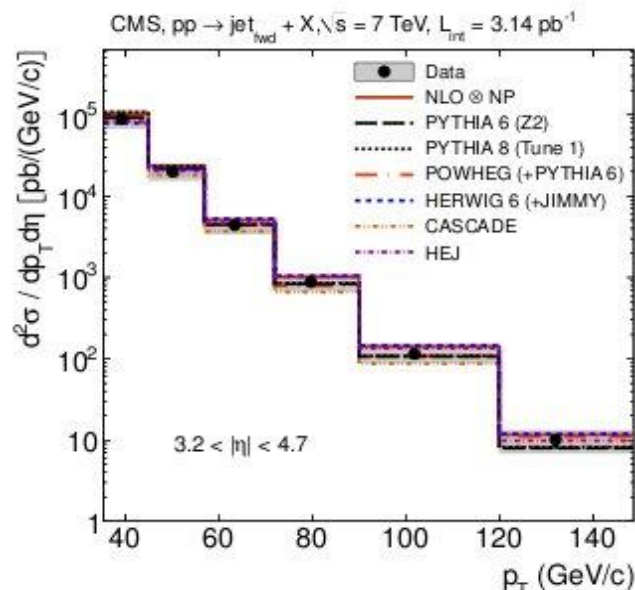
In small-x region standard approach to NLO QCD perturbative calculations. DGLAP (expansion in terms of power of $a_s \ln(Q^2)$) is predicted to be not sufficient. An alternative approach is BFKL (expansion in terms of $\ln(1/x)$).

Non perturbative effects, Multi Parton Interaction (MPI) etc. models have to be tuned to data.



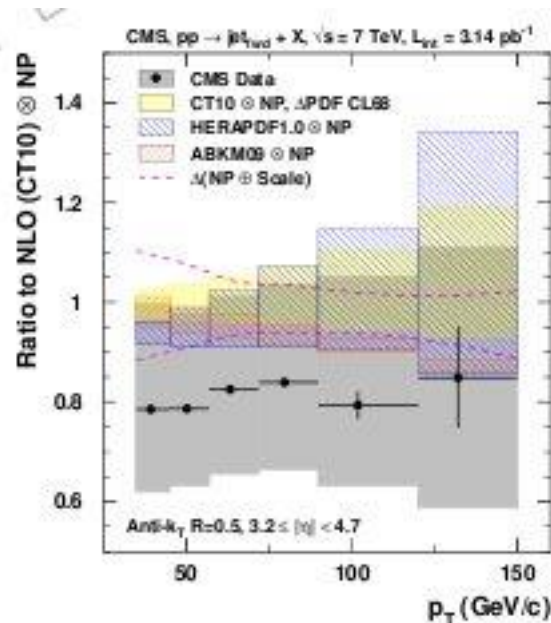
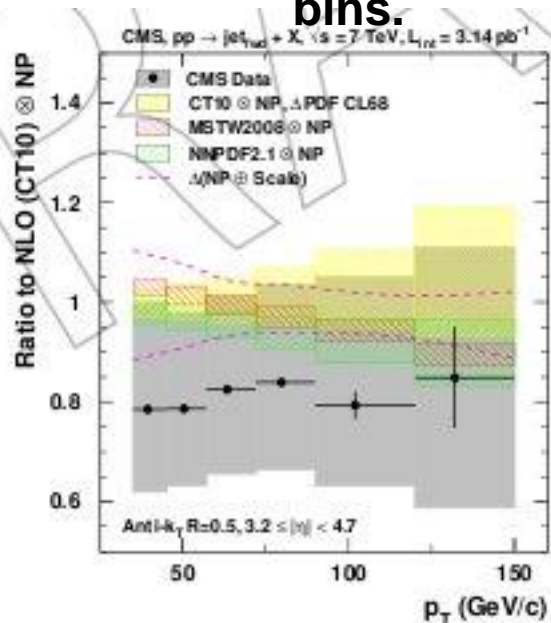
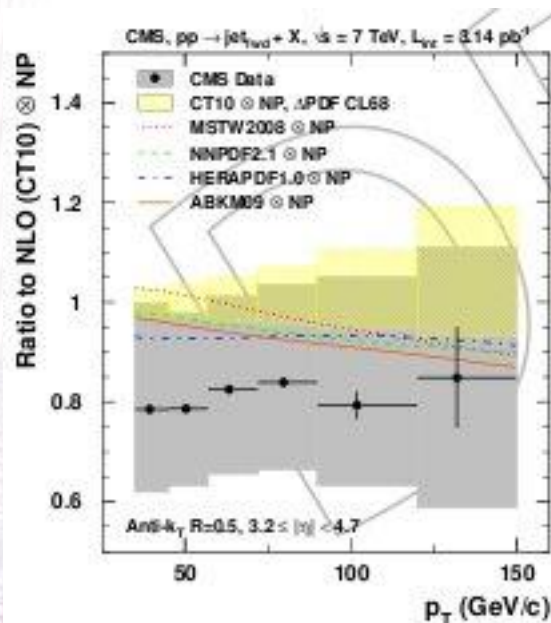
Inclusive forward jets at 7 TeV

Jet $3 < |\eta| < 5$

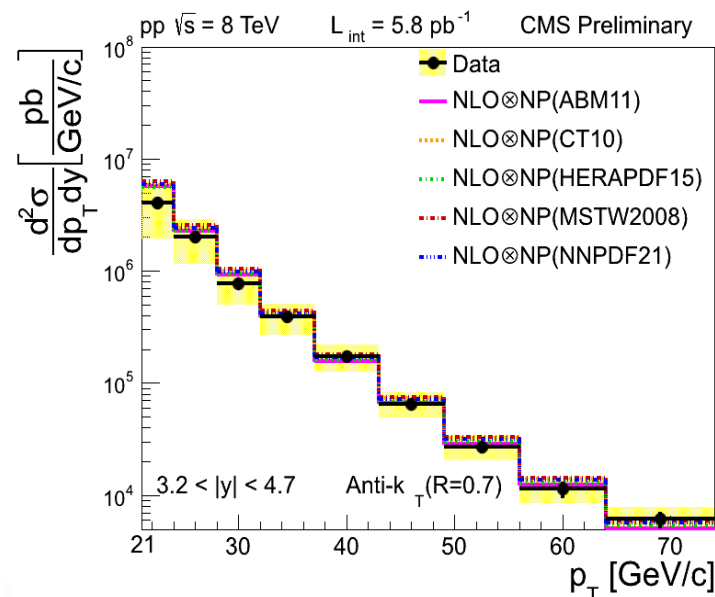
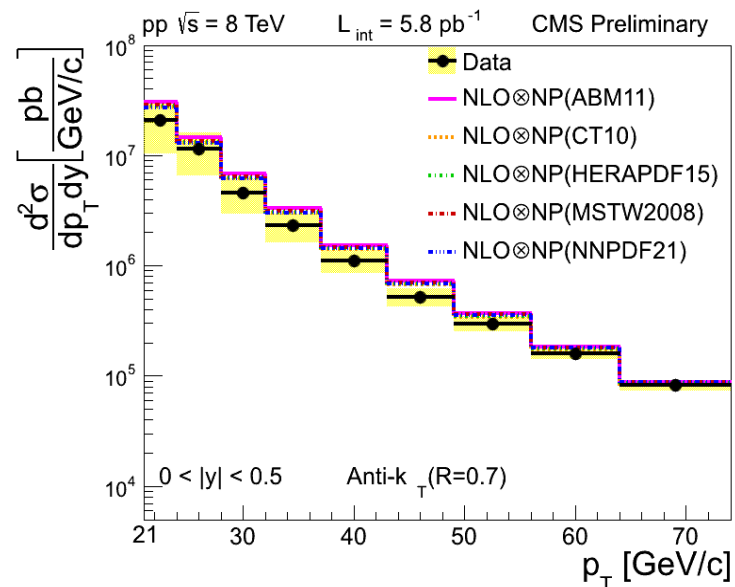
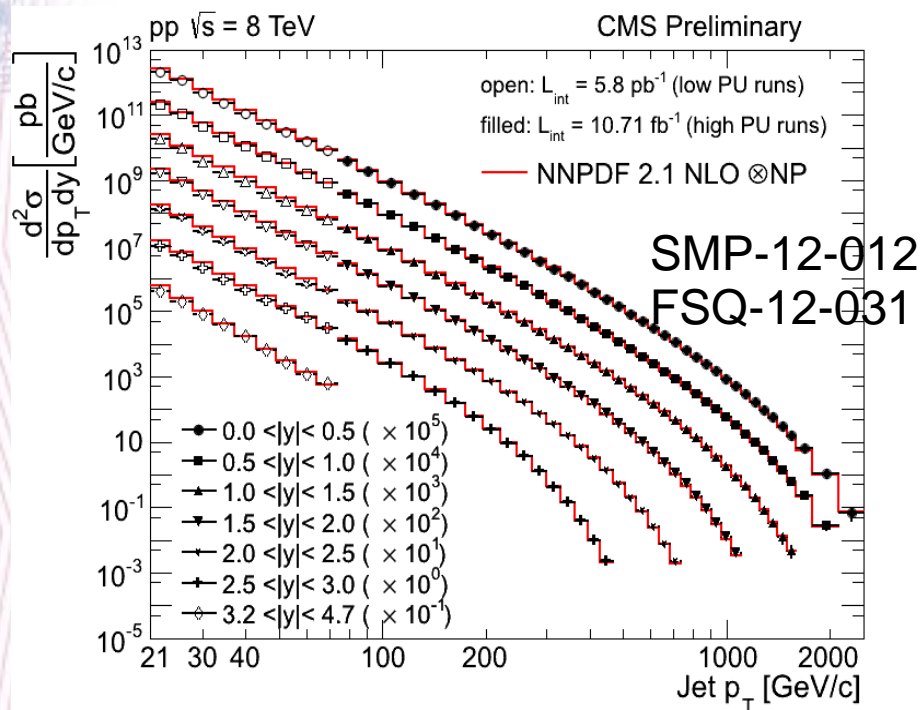


1. DGLAP evolution + parton showering (PYTHIA6/8, HERWIG 6) with the different UE tunes
DGLAP with angular ordered shower (HERWIG++ 2.3)
2. NLO (POWHEG)+PYTHIA6 or HERWIG 6
3. NLO (NLOJET++)+NP corrections
4. CCFM/BFKL evolution (CASCADE,HEJ) + uPDF

Data are in agreement with NLO calculations withing systematic uncertainties although NLO calculations are systematically overestimate cross-section in all rapidity bins.



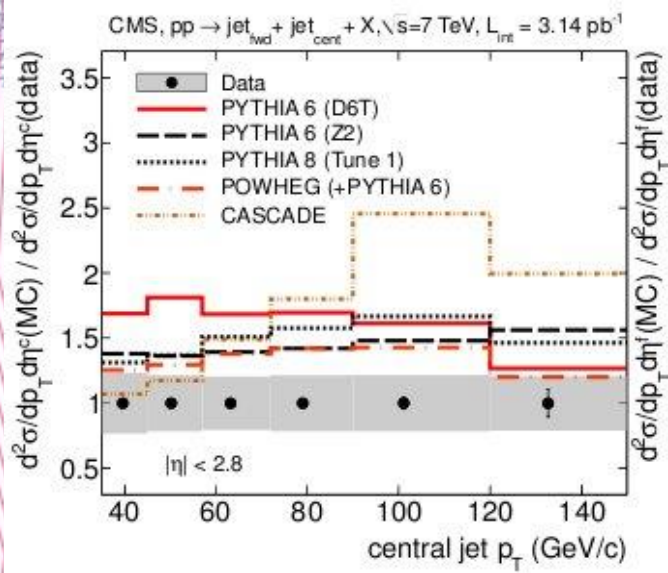
Low pt jets at 8 TeV



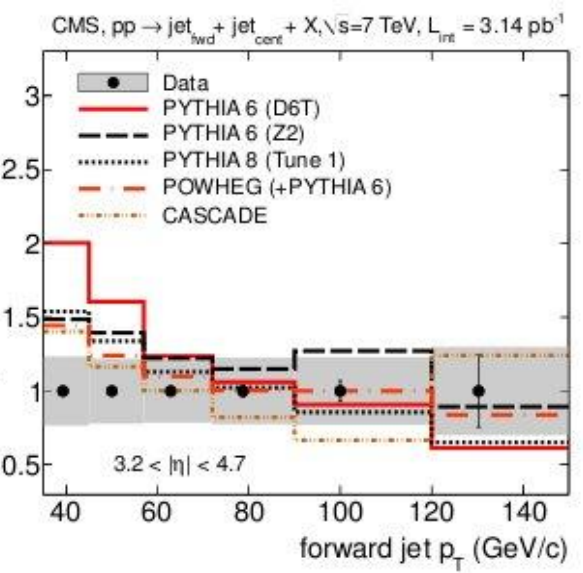
Theoretical predictions systematically overestimate x-section for both central and forward rapidity, but within experimental and theoretical uncertainties.

CMS-PAS-FSQ-12-031

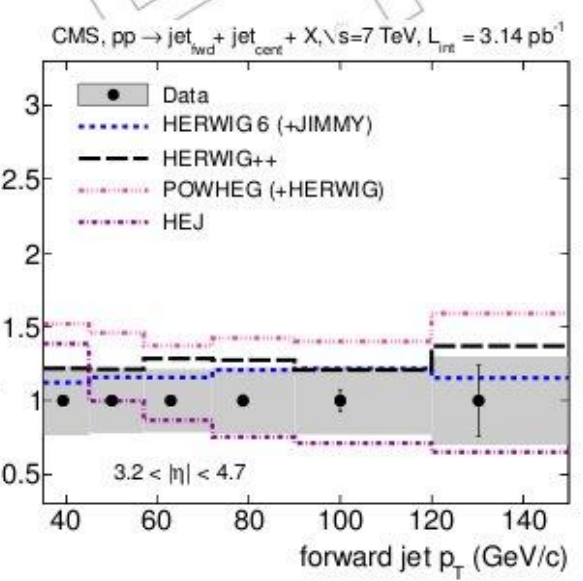
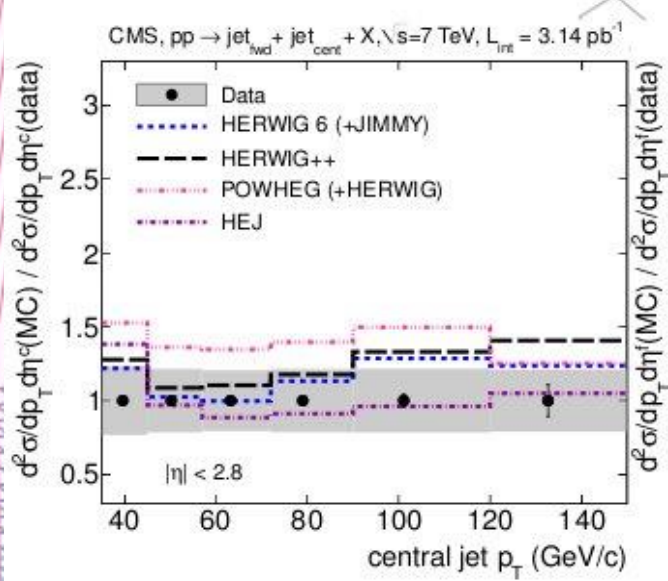
Central-forward dijets



(a)



(b)



One jet $|\eta| < 2.8$
 Second jet $3 < |\eta| < 5$

HERWIG6, HERWIG++ agrees both with central and forward jets flow

HEJ shows the reasonable agreement with dijet data

All PYTHIA tunes and NLO contributions from POWHEG overestimate data

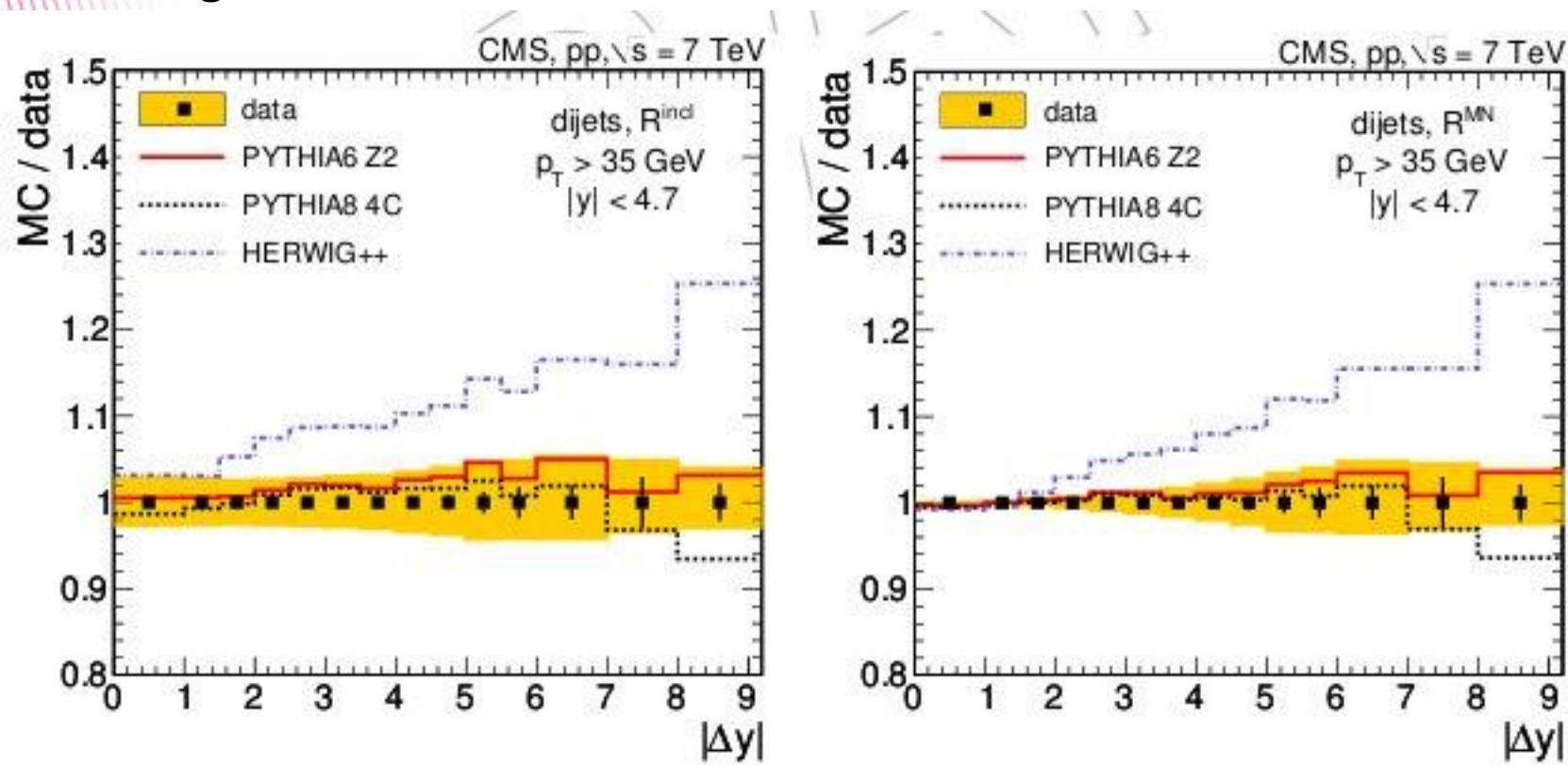
Valuable test of pQCD; possibility to constraint models

Dijet production vs Δy gap

$R_{inc} = \sigma(N_{jet} \geq 2) / \sigma(N_{jet} = 2)$
 R_{MN} (Mueller-Navelet dijets) – only jets with highest and lowest rapidities are considered

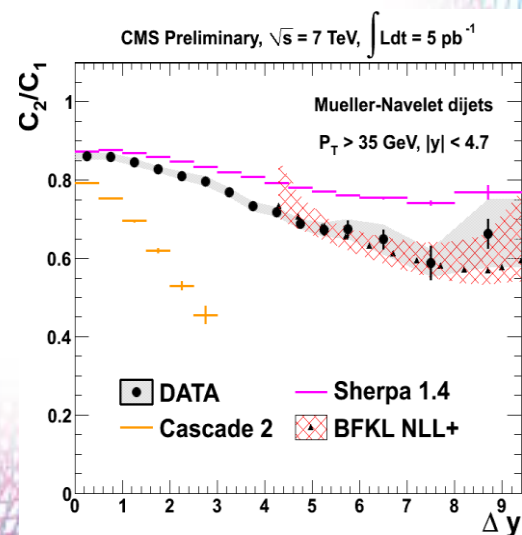
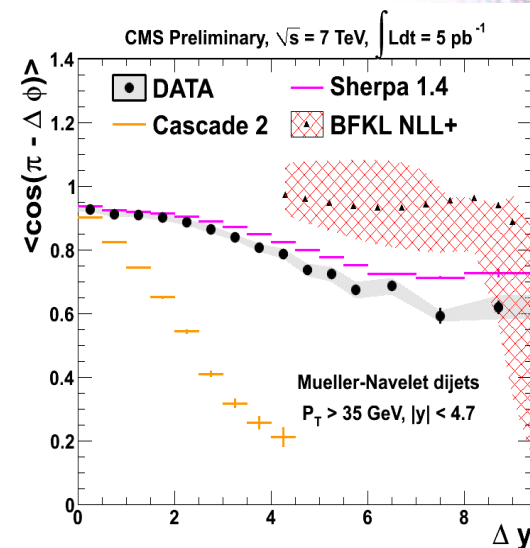
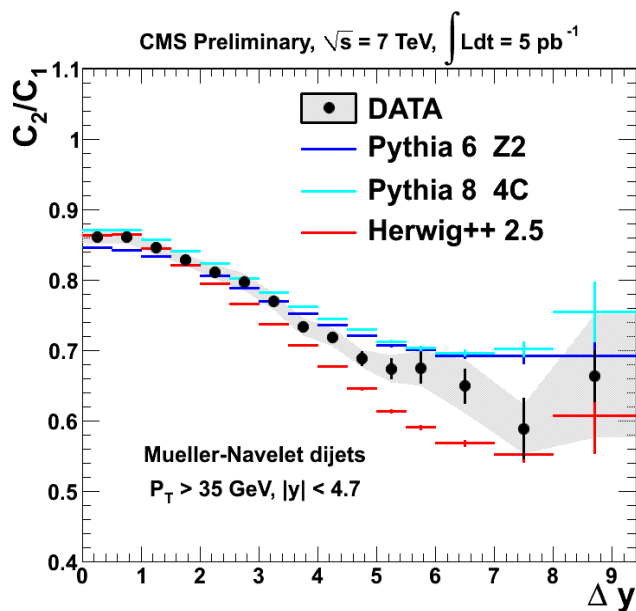
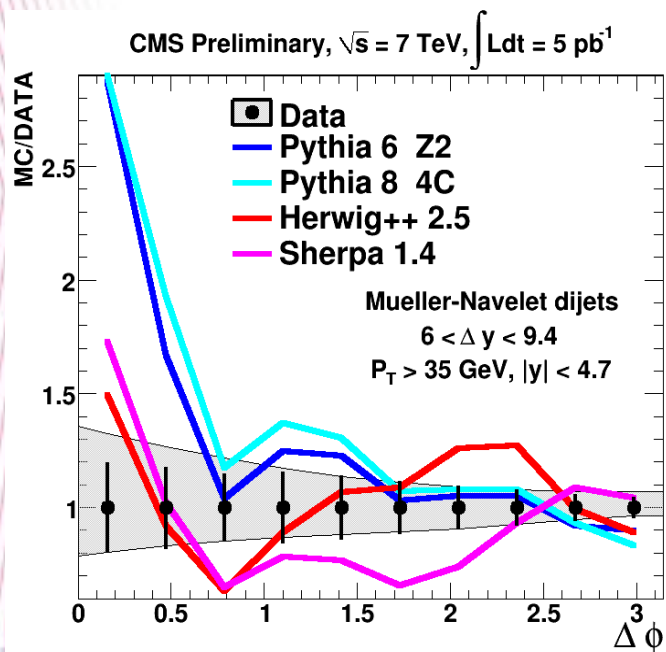
Probe small x regime:
 BFKL evolution:
 k_T factorization

PYTHIA MC agrees with data while HERWIG predicts higher MC ratio.
 BFKL motivated generators (CASCADE and HEJ+ARIADNE) predict significantly stronger rise than observed.



Angular correlations of jets

- Events with at least two jets passing cuts: $p_T > 35$ GeV in $|\eta| < 4.7$.
 - For a pair of jets with the largest $\Delta\eta$ (Mueller-Navelet dijet) the angular distance is calculated: $\Delta\phi = \phi_1 - \phi_2$
 - We study $\Delta\phi$ distributions for different $\Delta\eta$, and correlation factors C1, C2, C3 and its ratios $C_2/C_1, C_3/C_2$
- $$C_n(\Delta y, p_{Tmin}) = \langle \cos(n(\pi - \Delta\phi)) \rangle$$

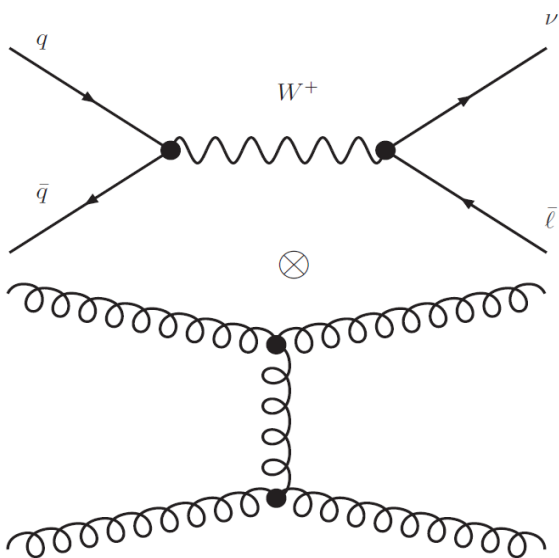


DGLAP generators starts to be worse in high Δy description
 BFKL/CCFM generators do not provide good description of data in full $\Delta\eta$ range.

Large unc. of NLL BFKL calculations.

[CMS-PAS-FSQ-12-002](#)

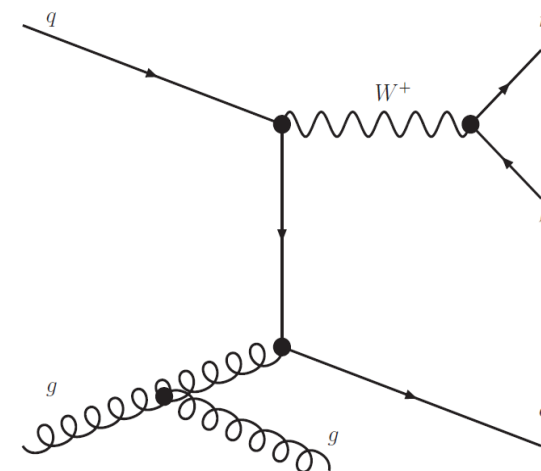
Double parton scattering



Double parton scattering

The measure of the size of DPS contribution

$$\sigma_{eff} = \frac{m \sigma_A * \sigma_B}{2 \sigma_{A+B}^{DPS}}$$

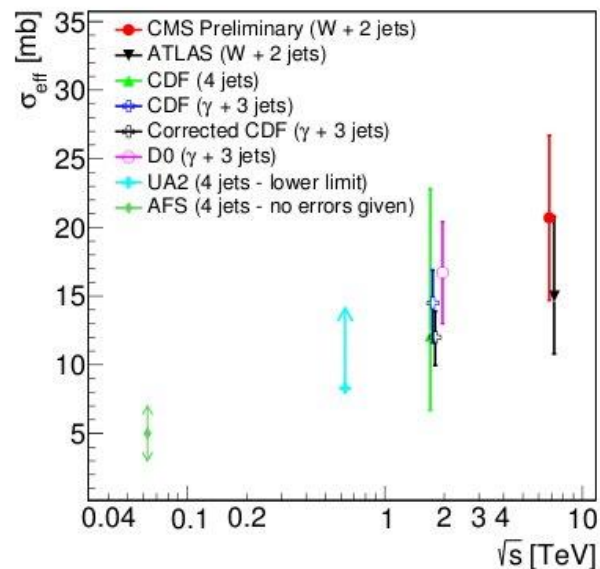


Single parton scattering

Template fit of the sensitive observables to find σ_{eff} :

$$\delta p_T = \frac{p_T(j1, j2)}{(p_T(j1) + p_T(j2))}$$

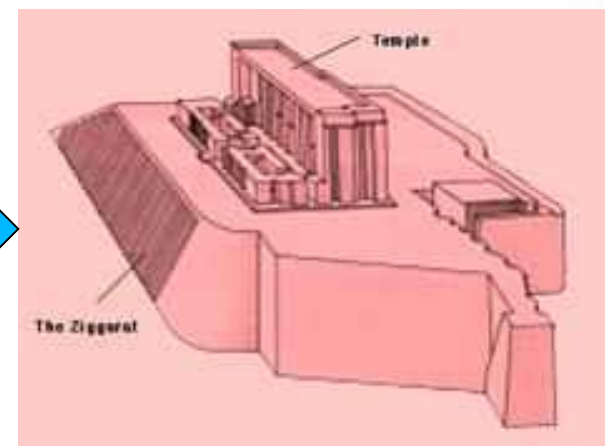
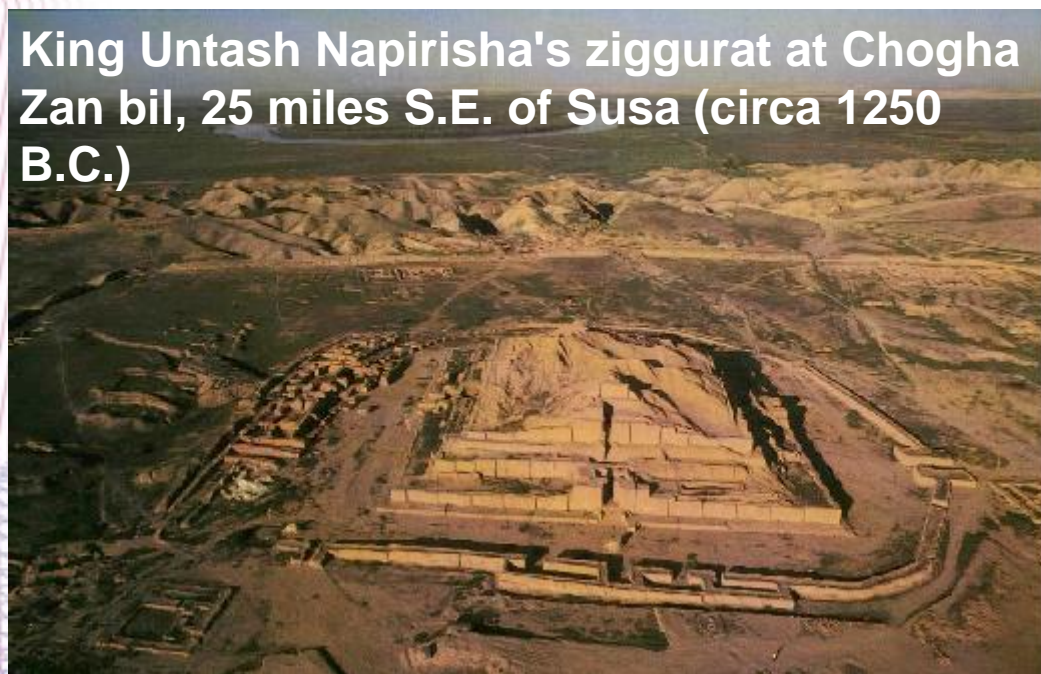
Azimuthal angle between W and dijet vector

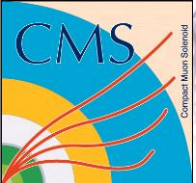


Summary

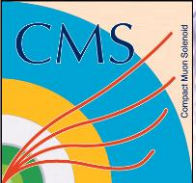
- CMS measures both hard and soft QCD processes in the different phase space regions comparing with the wide range of LO and NLO calculations
- The data are, in general, in broad agreement with the perturbative predictions, but enough discrepancies are observed to keep us busy for a while.

King Untash Napirisha's ziggurat at Chogha Zan bil, 25 miles S.E. of Susa (circa 1250 B.C.)





Thank you!

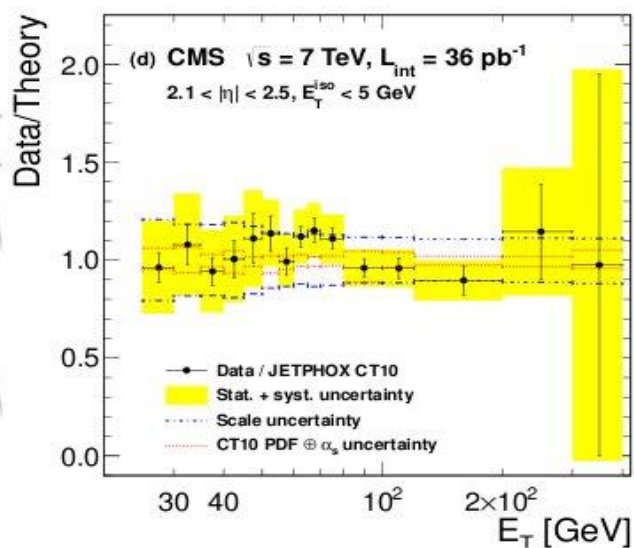
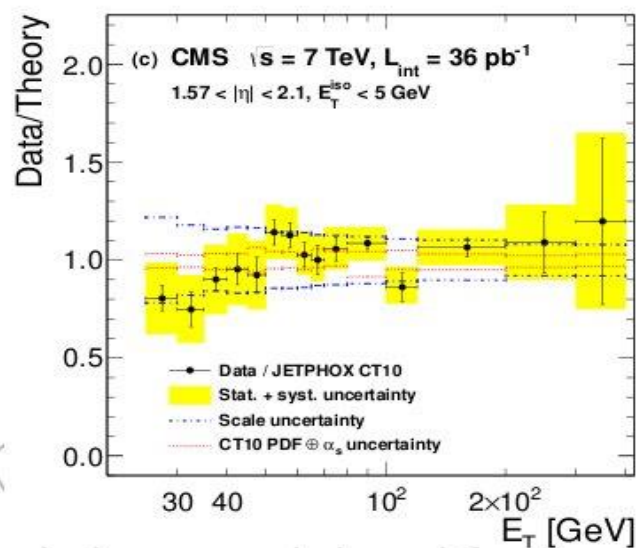
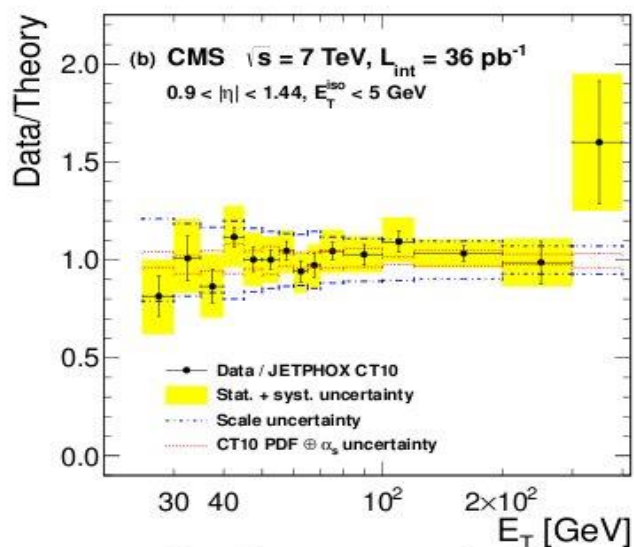
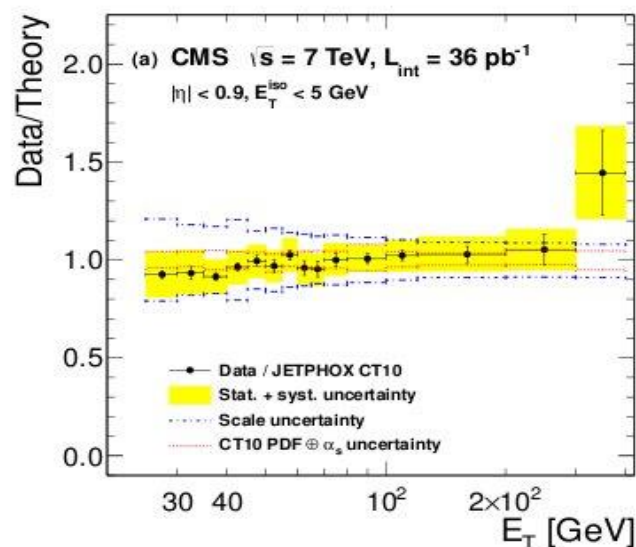


Bonus material

PDFs

- ❑ MSTW: global fit of hard scattering data with leading twist fixed order collinear factorization in the \overline{MS} scheme. Data: HERA DIS (except latest combined HERA-I data), fixed target DIS and DY, Tevatron jet, W, Z
- ❑ CTEQ: global fit of hard scattering data in the framework of general mass pQCD.
Data: same as MSTW (CT10 includes HERA-I+more Tevatron data)
- ❑ NNPDF: parametrize PDFs by training a neural network on MC replicas of the experimental data. Data: as above.
- ❑ HERAPDF: DGLAP evolution in the \overline{MS} scheme. QCD prediction for FF is done using convolution of PDFs with general mass variable flavor number RT scheme.
Data: NC and CC HERA DIS (v1.5), +HERA jets (v1.6)
- ❑ AB(K)M: Data: only NC (neutral current) DIS from HERA and fixed target
- ❑ GJR : dynamical approach for evolution. Data: DIS, DY, Tevatron jet data.

High- p_T photon production

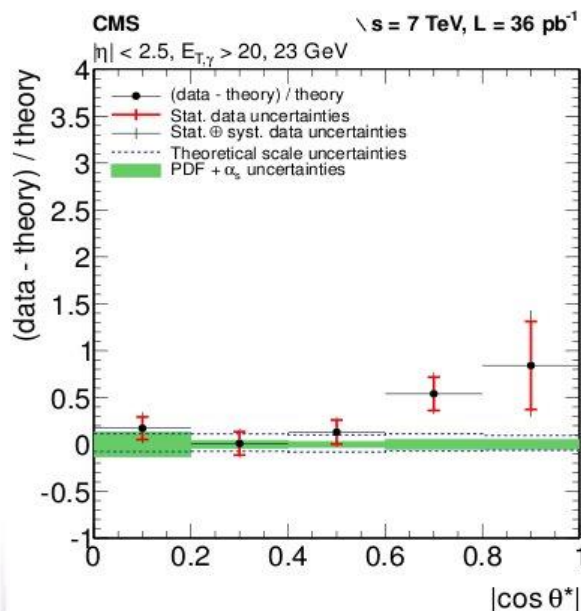
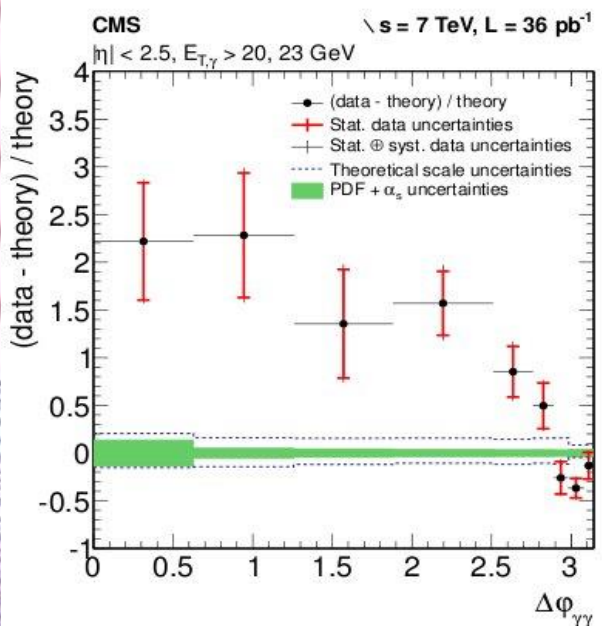
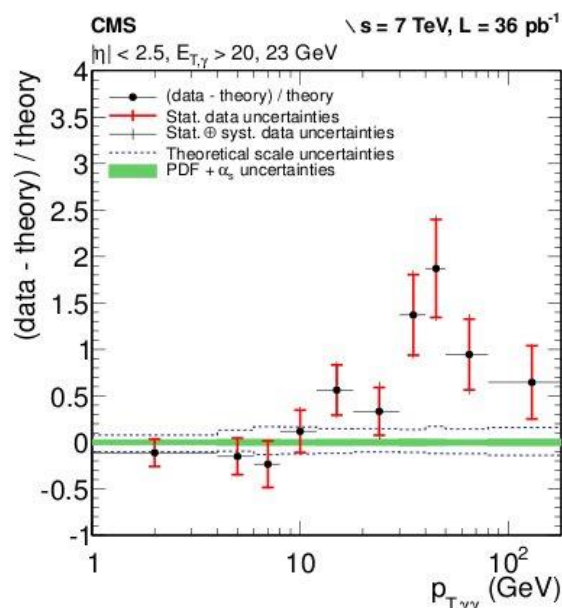
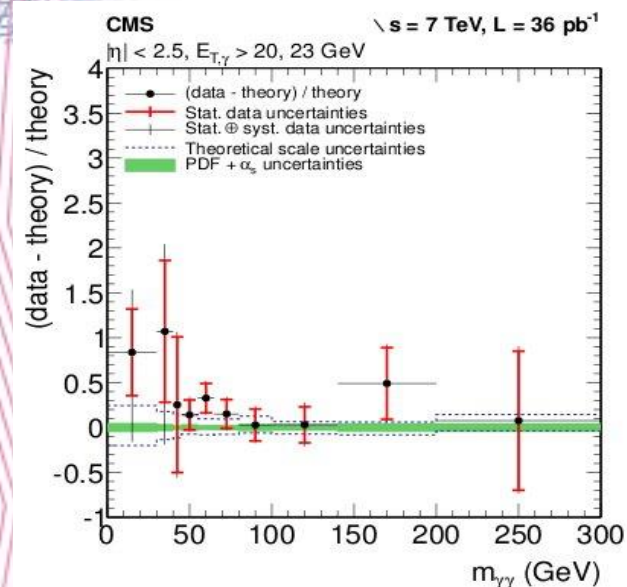


Bin-to-bin unfolding is performed

Predictions from the NLO pQCD (JETPHOX) agrees with Data except low p_T photons where NLO predictions tends to overestimated data.

PRD 84 052011 (2011)

Di-photon production



Unfolding to the particle level is done via Inverted matrix.

Annihilation: $q\bar{q} \rightarrow \gamma\gamma$

Fusion: $g g \rightarrow \gamma\gamma$

Fragmentation: $q g \rightarrow \gamma\gamma q$

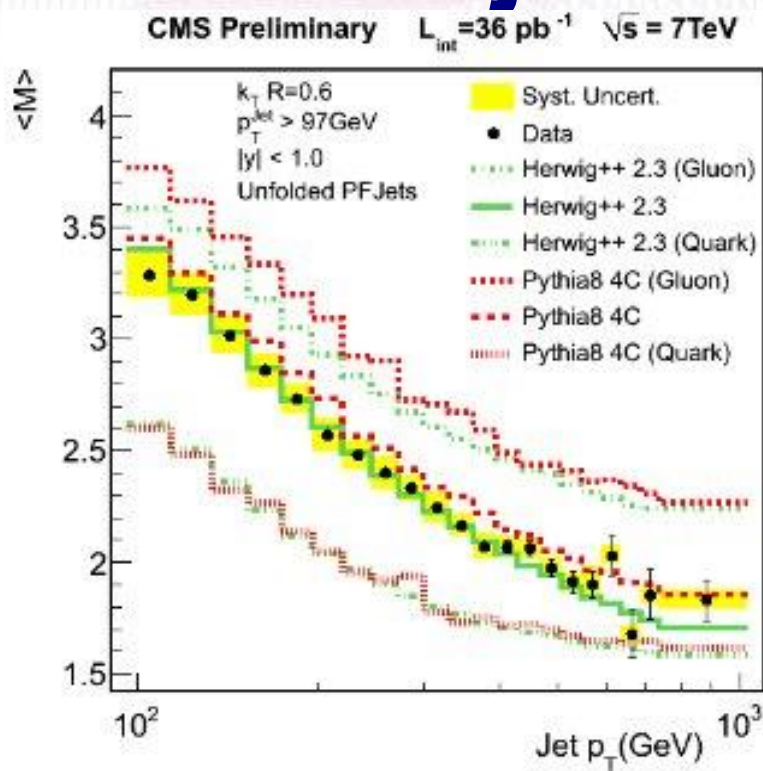
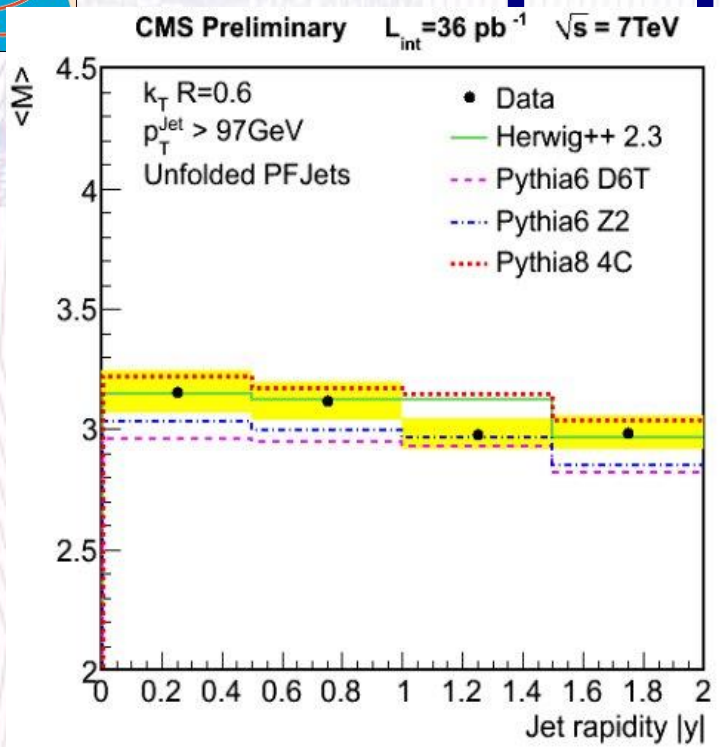
Calculation is done at NLO with DIPHOX, GAMMA2MC

The overall agreement in diphoton mass spectrum

The theoretical predictions underestimate the measured cross section for $\Delta\phi_{\gamma\gamma} < 2.8$

JHEP01(2012)133

Jet properties: subjets



K_T algorithm with parameter $R=0.6$ and a subjet resolution cutoff of $r=10^{-3}$ was used for subjet reconstruction

dAgostini Multidimensional unfolding method was used to unfold distributions to the particle level jets.

The average subjet multiplicity decreases with increasing jet p_T
 Fraction of the quark-induced jets increases with jet p_T and $|y|$
 The best agreement is achieved with HERWIG++ (but see previous slide – HERWIG++ gives the wrong shape in $\langle M \rangle$ plane)